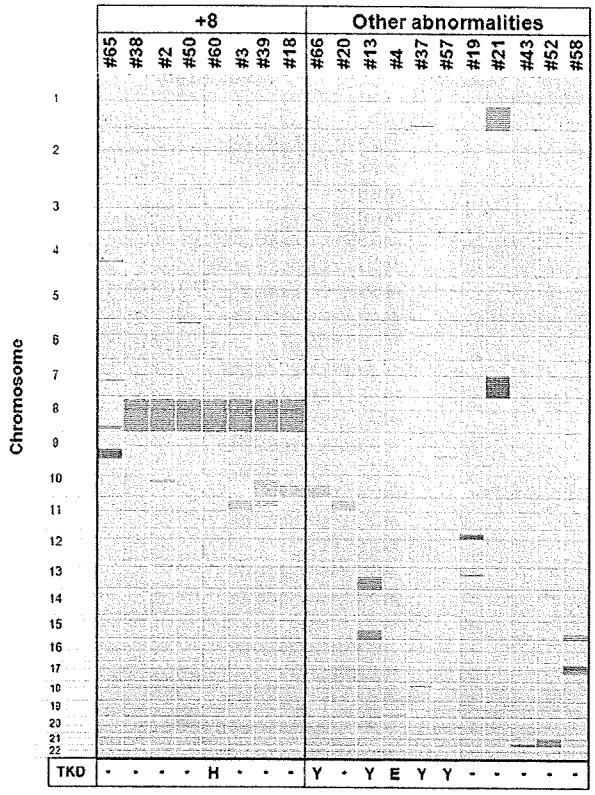

Figure 1. Summary of genomic abnormalities in t(15;17) APL samples. Genomic DNA of 47 t(15;17) APL samples were subjected to SNP-chip analysis, and genomic abnormalities are summarized. Color boxes are used to denote the type and size of abnormalities: pink (copy-number-neutral loss of heterozygosity; CNN-LOH); green (deletion); and red (duplication including trisomy). A total of 28 patients (60%) showed no detectable genomic abnormalities (data not shown). In contrast, 19 patients (40%) had one or more genomic abnormalities: trisomy 8 or duplication of the *MYC* gene region either with or without genomic abnormalities was found in 8 patients (17%, referred as "+8") and 11 patients (23%, referred as "other abnormalities") had genomic abnormalities without trisomy 8. Six patients (13%) had CNN-LOH; and 1 sample in +8 group and 5 samples in other abnormalities group had *FLT3* point mutations that are shown by their amino acid change at codon 835 from D (aspartic acid) to either Y (tyrosine), E (glutamic acid), or H (histidine).

no. 21 (1q21–q-terminal, 102.63 Mb), case no. 43 (21q22.12–q-terminal, 10.69 Mb), and case no. 58 (15q24.1–q-terminal, 27.97 Mb; and 17p11.2–q21.1, 14.05 Mb). The duplicated region at 21q of case no. 43 and at 17p of case no. 58 included the *ERG* and *ERBB2* genes, respectively. Importantly, the duplicated region at 8q of case no. 65 contained the *MYC* gene (Figure 2A). Seven cases had trisomy 8, and one of the candidate genes on chromosome 8 is the *MYC* gene; therefore, we classified case no. 65 within the +8 group.

Of note, the NB4 APL cell line had amplification of the *MYC* gene region (8q24.21), whereas the PL-21 APL cell line showed duplication of the region (Figure S2A). We compared levels of c-Myc mRNA in these cell lines, and found that NB4 cells had approximately 6-fold higher expression of c-Myc than did PL-21 cells (Figure S2B). This result indicated that copy-number change was associated with mRNA levels of the target gene.

CNN-LOH in t(15;17) samples

Several cases had the same chromosomal region involved in CNN-LOH. Chromosome 10q CNN-LOH was found in 3 cases (6%) including case no. 18 (10q22.2–q-terminal), case no. 39 (10q21.1–q-terminal), and case no. 66 (10q22.2–q-terminal; Figure 1; Figure S3A). This region included the tyrosine kinase receptor gene *FGFR2* and the tumor suppressor gene *PTEN* (Table 2). Cases no. 3, no. 20, and no. 39 had CNN-LOH on 11p-terminal–p11.12, 11p-terminal–p11.12, and 11p-terminal–p14.1, respectively; and the common region was 28.7 Mb (Figure 1; Figure S3B) containing the tumor suppressor genes *WT1* and *CDKN1C*, and the oncogene *HRAS* (Table 2). CNN-LOH of 19q13.2–q-terminal (17.3 Mb) occurred in one case (no. 4, Table 2).

Comparison of chromosomal changes between diagnosis and complete remission samples

To assess whether chromosomal alterations detected by SNP-chip analysis were acquired abnormalities, germ-line mutations, or copy-number variants, we compared chromosomal changes between diagnosis and complete remission (CR) samples in the same patients. CR samples of cases no. 2, no. 3, no. 18, no. 19, no. 38, no. 39, and no. 50 were available, and these CR samples were subjected to SNP-chip analysis. As shown in Figure 4, trisomy 8 of case no. 2 and CNN-LOH of case no. 18 at diagnosis were not present in the samples obtained at CR. Other alterations including trisomy 8 (cases no. 3, no. 18, no. 38, no. 39, and no. 50), CNN-LOH at chromosomes 10 (case no. 39) and 11 (cases no. 3 and no. 39), and deletions (cases no. 2, no. 19, and no. 50) also were not present at CR (Figure S4). Taken together, these results showed that chromosomal alterations detected by SNP-chip analysis were acquired somatic changes.

Relationship between genomic abnormalities and FLT3 mutations

Finally, we compared genomic abnormalities and *FLT3* status. Twenty-four samples (51%) had wild-type *FLT3;* whereas 12 samples (26%) had *FLT3*-TKD mutation (aspartic acid at codon 835, D835) and another 11 samples (23%) had *FLT3*-ITD form. Interestingly, all 11 samples with *FLT3*-ITD were found only in the normal-copy-number (NC) group (Tables 1 and 3). One sample in the trisomy 8 group had a *FLT3*-TKD mutation. Samples in the "other abnormalities" group did not have *FLT3*-ITD; and 6 samples in NC group and 5 samples in the "other abnormalities" group had a *FLT3*-TKD mutation. These results suggested that the pathway of development of APL differs in each group; in a mutually exclusive fashion, *FLT3*-ITD, trisomy 8, and unknown factor(s) were involved in each group.

Discussion

Our genome-wide SNP-chip analysis showed that 40% of t(15;17) APL samples had one or more genomic abnormalities including deletions, duplications, and/or CNN-LOH. Since the PML-RARα fusion protein is probably not sufficient to cause APL in murine model systems, the additional genetic changes that we found may be necessary to cause the leukemia.

Our analysis revealed that 6 samples (13%) of t(15;17) APL samples had CNN-LOH. Previously, we analyzed AML with normal karyotype samples and found that 32% of cases had CNN-LOH (Akagi et al[28]); and other investigators also demonstrated CNN-LOH in AML samples at a frequency of 15% to 20%.[22-25,27] Of interest, approximately 40% of relapse AML had CNN-LOH.[26] CNN-LOH in t(15;17) APL is about half as frequent as the other AMLs. Two CNN-LOH regions occurred in multiple samples: chromosomes 10q (58.2 Mb, 3 cases) and 11p (28.7 Mb, 3 cases). Of note, case no. 39 had both 10q and 11p CNN-LOHs, suggesting that 10q and 11p might contain novel APL-related gene(s). CNN-LOH is a genomic abnormality that

Table 2. Chromosomal alterations in t(15;17) APL samples

Group/case no.	Status	Location	Physical localization		Size, Mb	Gene(s) in the region
			Proximal	Distal		
+8						
65	Del	4q28.1	125 190 507	126 521 903	1.33	*KIAA1223*
	Del	7q21.11-q21.12	85 414 972	86 445 002	1.03	*GRM3, KIAA1324L,* and *DMTF1*
	Dup	8q24.13-q24.22	122 607 785	132 092 760	9.48	> 10 genes including *MYC*
	Del	9q12-q31.3	64 207 745	111 479 523	47.27	> 10 genes
38	Tri	Trisomy 8				
2	Tri	Trisomy 8				
	Del	10q21.2-q21.3	62 496 958	68 046 104	5.55	>10 genes
50	Del	6p25.1-p24.3	5 545 437	8 054 930	2.51	> 10 genes
	Tri	Trisomy 8				
60	Tri	Trisomy 8				
3	Tri	Trisomy 8				
	CNN-LOH	11p.ter–p11.12	1 938 894	49 879 899	47.9	> 10 genes including *WT1, CDKN1C* and *HRAS*
39	Tri	Trisomy 8				
	CNN-LOH	10q21.1–q-ter	59 576 047	135 228 726	75.7	> 10 genes including *PTEN* and *FGFR2*
	CNN-LOH	11p.ter–p14.1	1 938 894	30 627 880	28.7	> 10 genes including *CDKN1C* and *HRAS*
18	Tri	Trisomy 8				
	CNN-LOH	10q22.2–q-ter	76 995 152	135 228 726	58.2	> 10 genes including *PTEN* and *FGFR2*
Other						
66	CNN-LOH	10q22.2–q-ter	76 289 513	135 295 604	59.0	> 10 genes including *PTEN* and *FGFR2*
20	CNN-LOH	11p.ter–p11.12	1 938 894	49 330 228	47.4	> 10 genes including *WT1, CDKN1C* and *HRAS*
13	Dup	13q21.1–q-ter	56 784 440	114 051 465	57.27	> 10 genes
	Dup	15q22.2–q-ter	57 244 668	100 182 183	42.94	> 10 genes including *PML*
4	CNN-LOH	19q13.2–q-ter	46 160 099	63 437 743	17.3	> 10 genes
37	Del	1q42.2	227 843 862	227 867 765	0.02	*EGLN1*
	Dup	18p11.31-p11.23	7 192 739	7 657 575	0.46	*PTPRM*
57	Dup	9q22.32	94 435 025	94 710 006	0.27	*FBP2, FBP1,* and *C9orf3*
19	Del	12p13.31-p11.22	6 755 671	29 248 257	22.49	> 10 genes including *ETV6* and *CDKN1B*
	Del	13q14.2-q14.3	49 630 676	50 510 777	0.88	*FAM10A4, DLEU7, FLJ11712,* and *GUCY1B2*
21	Dup	1q21–q-ter	142 487 224	245 120 412	102.63	> 10 genes
	Del	7q11.21–q-ter	61 522 282	158 554 645	97.03	> 10 genes
43	Dup	21q22.12–q-ter	36 234 195	46 924 583	10.69	>10 genes including *ERG*
52	Tri	Trisomy 21				
58	Dup	15q24.1–q-ter	72 224 840	100 192 115	27.97	> 10 genes
	Del	17p-ter–p11.2	18 901	21 459 693	21.44	> 10 genes including *TP53*
	Dup	17p11.2-q21.1	21 491 135	35 542 587	14.05	> 10 genes including *NF1* and *ERBB2*

Physical localization, size (Mb), and gene(s) at the chromosomal regions were obtained from UCSC Genome Browser. If known gene(s) in the chromosomal regions are less than 10, all gene names are displayed.

Copy number changes as previously described as copy number variant at Database of Genomic Variants (http://projects.tcag.ca/variation/)[29] and UCSC Genome Browser (http://genome.ucsc.edu/)[32] were excluded.

Del indicates deletion; Dup, duplication; Tri, trisomy; ter, terminal; and CNN-LOH, copy-number-neutral loss of heterozygosity.

normally cannot be detected by conventional cytogenetic analysis. These regions usually contain a mutation of a key gene. For example, a constitutively active form of either *JAK2* V617F mutant, *FLT3*-ITD, *AML1/RUNX1* frameshift, and/or mutations of *WT1* and *NPM1* were found in CNN-LOH regions in AML.[22-25] CNN-LOH regions identified in this study contain genes coding for several tyrosine kinase and/or tumor suppressors. Further studies are required to identify the key dysregulated gene(s) in these regions. In addition to CNN-LOH, we also found several copy-number changes that may be sites containing novel disease-related genomic regions in t(15;17) APL. Although we cannot rule-out copy-number variants (CNVs) at several sites, we think it is unlikely. We had 7 genomic DNA at complete remission samples and confirmed for each that the chromosomal changes were only in the leukemia cells. Furthermore, for each of these sites, we interrogated a collated library of CNVs (Database of Genomic Variants and UCSC Genome Browser) to assure that these regions were not known CNVs.

FLT3 is a tyrosine kinase receptor involved in normal hematopoiesis, and mutations of the gene often occur in AML. Incidence of *FLT3*-ITD and *FLT3*-TKD was 23% and 26% in our samples, respectively. Experiments have shown that *FLT3*-ITD and *FLT3*-TKD have differences in their downstream signaling.[33-35] Interestingly, bone marrow transplantation in mice showed that *FLT3*-ITD induced an oligoclonal myeloproliferative disease,[33] whereas *FLT3*-TKD produced an oligoclonal lymphoid disorder with a long latency.[34] Furthermore, only *FLT3*-ITD caused activation of STAT5 and repression of C/EBPα and PU.1.[34,35]

Here, t(15;17) APL samples were divided into 3 groups based on genomic status detected by SNP-chip analysis: normal-copy-number group (NC group, 28 samples); trisomy 8 group (+8 group, 8 samples); and other abnormalities group (11 samples). Notably, our subclassifications did reveal an interesting relationship between genomic status and *FLT3* mutation. Eleven samples of NC group (39% of the NC group samples) had *FLT3*-ITD, whereas no *FLT3*-ITD occurred in samples from the other 2 groups. In contrast, one good candidate gene in the +8 cohort is the oncogene *MYC*. In fact, case no. 65 had duplication localized to 8q24.13-q24.22 that included the

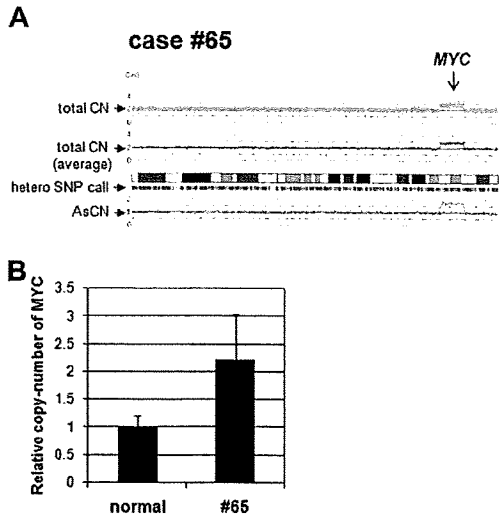

Figure 2. Validation of copy-number change in case no. 65. (A) SNP-chip data of chromosome 8 in case no. 65. Top dots are SNP sites as probes and indicate total copy number (CN). Middle line is an average of the copy number and shows gene dosage. Bars are heterozygous (hetero) SNP calls. Bottom 2 lines show allele-specific copy number (AsCN). (B) Duplication of the *MYC* gene region in case no. 65. Copy number of the *MYC* gene in case no. 65 was compared with normal genomic DNA with quantitative genomic real-time PCR. Level of the copy number was determined as a ratio between the *MYC* gene and the reference genomic region 2p21. Results represent mean of 3 experiments plus or minus SD.

MYC gene. Previous karyotype analysis showed that the PL-21 cell line, which was established from an APL patient, had a polyploid male karyotype with 13q+ chromosome, but a translocation between chromosome 15 and 17 was not identified.[36] NB4 cells are cytogenetically very complex, with a hypotetraploid karyotype and multiple chromosomal alterations.[37,38] Our SNP-chip analysis of NB4 cells also showed ploidy = 3.67, indicating that the karyotype is hypotetraploid. Of interest, NB4 cells have amplification of the *MYC* gene. Importantly, expression of c-Myc mRNA is stimulated by *FLT3*-ITD[39,40]; and AML samples with *FLT3*-ITD have increased expression of c-Myc mRNA compared with normal bone marrow.[41] These data indicate that the *MYC* gene may be dysregulated by either copy-number change or *FLT3*-ITD as a secondary abnormality to enhance the development of APL. Of course, our sample population is small, therefore, additional studies are needed to confirm these findings.

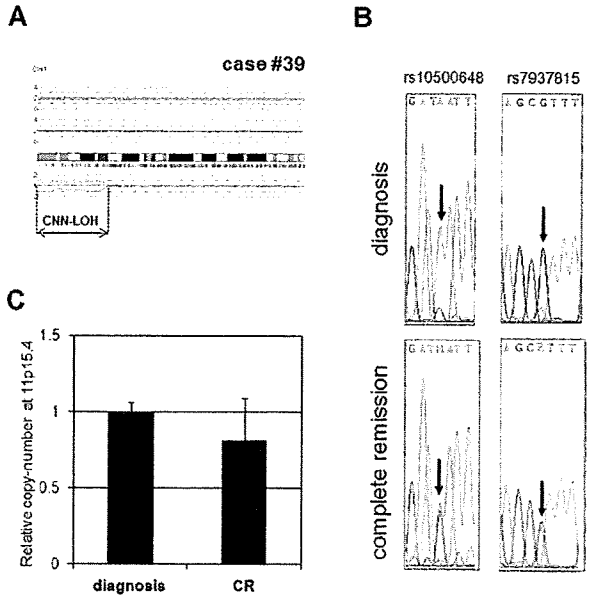

Figure 3. Validation of CNN-LOH in case no. 39. (A) SNP-chip data of chromosome 11 in case no. 39. The samples had CNN-LOH on chromosome 11 (11p-terminal–p14.1, 28.7 Mb). (B) Determination of SNP sequence in 11p CNN-LOH region in case no. 39. 2 SNP sites (rs10500648 and rs7937815) were sequenced. Both SNP sites showed heterozygosity in the complete remission sample, whereas they showed homozygosity in the diagnosis sample. (C) Determination of copy number in the 11p15.4 region. Copy number of 11p15.4 (CNN-LOH region) in case no. 39 at diagnosis was compared with complete remission (CR) sample with quantitative genomic real-time PCR. Levels of the copy number were determined as a ratio between 11p15.4 and the reference genomic DNA, 2p21. Results represent the mean of 3 experiments plus or minus SD.

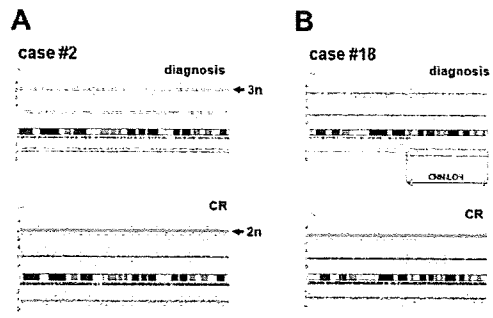

Figure 4. Comparison of chromosomal changes between diagnosis and complete remission samples. (A) Trisomy 8 in case no. 2. Case no. 2 had trisomy 8 at diagnosis, whereas chromosome 8 was 2n at complete remission (CR). (B) CNN-LOH in case no. 18. Case no. 18 had CNN-LOH in chromosome 10 (10q22.2–q-terminal, 58.2 Mb), and the alteration was not present in the matched CR sample.

Our APL cohort "other abnormalities" group has neither *FLT3*-ITD nor trisomy 8, but has several other genomic changes including deletion of *ETV6/TEL* (case no. 19) and duplication of *ERG* (case no. 43). ETV6/TEL is a transcriptional repressor, and approximately 30% of AML patients have loss of expression of ETV6/TEL protein.[42,43] In addition, mutation of the *ETV6/TEL* gene occurs in approximately 2% of AML samples, and these mutants behaved in a dominant-negative fashion.[43] ERG is a member of the ETS family of transcription factors and is a proto-oncogene. Overexpression of ERG predicts a worse outcome in AML with normal karyotype.[44] Taken together, our observed copy-number changes in these regions may be involved in development of APL.

Our findings extend those of Le Beau et al[13] who recently reported elegant models of APL using transgenic mice coexpressing PML-RARα and either BCL2, IL3, activated IL3R, or activated murine FLT3 ($FLT3^{W51}$). *PML-RARα/BCL2* mice developed leukemia, and these cells had a complex karyotype including trisomy 15 (100% of these mice), where the oncogene *MYC* is located. In contrast, *PML-RARα/FLT3*^{W51} mice develop

Table 3. Relationship between chromosomal abnormality and *FLT3* mutations

	Group			Total (%), 47 (100%)
	NC, 28 (60%)	+8, 8 (17%)	Other, 11 (23%)	
*FLT3*WT	11	7	6	24 (51)
*FLT3*TKD	6	1	5	12 (26)
*FLT3*ITD	11	0	0	11 (23)

Mutational status of the *FLT3* gene is shown.

NC indicates normal-copy-number; +8, trisomy 8 or duplication of the *MYC* gene region; other, other abnormalities; and WT, wild-type.

leukemia, and these cells had normal karyotype except for trisomy of either chromosomes 8 (29%), 10 (43%), or 15 (43%), and monosomy X (86%). These models suggest that different cooperating events are involved in the development of murine APL. Taken together, these findings strongly suggest that the pathway of development of APL differs in each of our cohorts; *FLT3*-ITD, *MYC*, and unknown factor(s) are involved in the development of APL; and these finding should facilitate the screening for novel therapeutic targets in each case.

Further studies in a larger cohort of patients will begin to stratify prognostically the APL patients in relation to the genomic changes of their leukemic cells; and new therapeutic targets, which are involved in the development of APL, should be discovered.

Acknowledgments

We thank members of our laboratory for helpful discussions. APL cell line PL-21 was kindly provided by Dr Ikezoe Takayuki (Kochi University, Kochi, Japan).

This work was supported by National Institutes of Health (NIH, Bethesda, MD) grant 5R01CA026038-30 (H.P.K.), the Inger Foundation, (Greenwich, CT), the Tom Collier Memorial Regatta Foundation (Los Angeles, CA), the Parker Hughes Fund (Los Angeles, CA), as well as grant NHRI-EX96-9434SI (National Health Research Institutes, Miaoli, Taiwan; L.-Y.S.) and grant MMH-E-96009 (Mackay Memorial Hospital, Taipei, Taiwan; D.-C.L.). H.P.K. is the holder of the Mark Goodson endowed Chair in Oncology Research and is a member of the Jonsson Cancer Center and the Molecular Biology Institute, UCLA. The study is dedicated to David Golde, a mentor and friend.

Authorship

Contribution: T.A. performed research, analyzed the data, and wrote the paper; M.K., S.O., G.Y., and M.S. performed SNP-chip analysis and developed CNAG; N.K., R.O., and C.W.M. assisted in data analysis; L.-Y.S. and D.-C.L. provided APL samples and clinicohematologic data for all APL patients, and performed *FLT3* mutation analysis; and H.P.K. directed the overall study.

Conflict-of-interest disclosure: The authors declare no competing financial interests.

Correspondence: Tadayuki Akagi, Department of Stem Cell Biology, Graduate School of Medical Science, Kanazawa University, 13-1 Takara-machi, Kanazawa, Ishikawa 920-8640, Japan; e-mail: tadayuki@staff.kanazawa-u.ac.jp.

References

1. de Thé H, Chomienne C, Lanotte M, Degos L, Dejean A. The t(15;17) translocation of acute promyelocytic leukaemia fuses the retinoic acid receptor alpha gene to a novel transcribed locus. Nature. 1990;347:558-561.
2. de Thé H, Lavau C, Marchio A, Chomienne C, Degos L, Dejean A. The PML-RAR-alpha fusion mRNA generated by the t(15;17) translocation in acute promyelocytic leukemia encodes a functionally altered RAR. Cell. 1991;66:675-684.
3. Grignani F, De Matteis S, Nervi C, et al. Fusion proteins of the retinoic acid receptor-alpha recruit histone deacetylase in promyelocytic leukaemia. Nature. 1998;391:815-818.
4. Warrell RP Jr, de The H, Wang ZY, Degos L. Acute promyelocytic leukemia. N Engl J Med. 1993;329:177-189.
5. Melnick A, Licht JD. Deconstructing a disease: RARalpha, its fusion partners, and their roles in the pathogenesis of acute promyelocytic leukemia. Blood. 1999;93:3167-3215.
6. Grisolano JL, Wesselschmidt RL, Pelicci PG, Ley TJ. Altered myeloid development and acute leukemia in transgenic mice expressing PML-RAR alpha under control of cathepsin G regulatory sequences. Blood. 1997;89:376-387.
7. Brown D, Kogan S, Lagasse E, et al. A PML-RARalpha transgene initiates murine acute promyelocytic leukemia. Proc Natl Acad Sci U S A. 1997;94:2551-2556.
8. Reilly JT. Class III receptor tyrosine kinases: role in leukaemogenesis. Br J Haematol. 2002;116:744-757.
9. Callens C, Chevret S, Cayuela JM, et al. Prognostic implication of FLT3 and Ras gene mutations in patients with acute promyelocytic leukemia (APL): a retrospective study from the European APL Group. Leukemia. 2005;19:1153-1160.
10. Bowen DT, Frew ME, Hills R, et al. RAS mutation in acute myeloid leukemia is associated with distinct cytogenetic subgroups but does not influence outcome in patients younger than 60 years. Blood. 2005;106:2113-2119.
11. Sohal J, Phan VT, Chan PV, et al. A model of APL with FLT3 mutation is responsive to retinoic acid and a receptor tyrosine kinase inhibitor, SU11657. Blood. 2003;101:3188-3197.
12. Chan IT, Kutok JL, Williams IR, et al. Oncogenic K-ras cooperates with PML-RAR alpha to induce an acute promyelocytic leukemia-like disease. Blood. 2006;108:1708-1715.
13. Le Beau MM, Bitts S, Davis EM, Kogan SC. Recurring chromosomal abnormalities in leukemia in PML-RARA transgenic mice parallel human acute promyelocytic leukemia. Blood. 2002;99:2985-2991.
14. Kelly LM, Kutok JL, Williams IR, et al. PML/RARalpha and FLT3-ITD induce an APL-like disease in a mouse model. Proc Natl Acad Sci U S A. 2002;99:8283-8288.
15. Nannya Y, Sanada M, Nakazaki K, et al. A robust algorithm for copy number detection using high-density oligonucleotide single nucleotide polymorphism genotyping arrays. Cancer Res. 2005;65:6071-6079.
16. Engle LJ, Simpson CL, Landers JE. Using high-throughput SNP technologies to study cancer. Oncogene. 2006;25:1594-1601.
17. Yamamoto G, Nannya Y, Kato M, et al. Highly sensitive method for genomewide detection of allelic composition in nonpaired, primary tumor specimens by use of affymetrix single-nucleotide-polymorphism genotyping microarrays. Am J Hum Genet. 2007;81:114-126.
18. Pfeifer D, Pantic M, Skatulla I, et al. Genome-wide analysis of DNA copy number changes and LOH in CLL using high-density SNP arrays. Blood. 2007;109:1202-1210.
19. Lehmann S, Ogawa S, Raynaud SD, et al. Molecular allelokaryotyping of early-stage, untreated chronic lymphocytic leukemia. Cancer. 2008;112:1296-305.
20. Mullighan CG, Goorha S, Radtke I, et al. Genome-wide analysis of genetic alterations in acute lymphoblastic leukaemia. Nature. 2007;446:758-764.
21. Kawamata N, Ogawa S, Zimmermann M, et al. Molecular allelokaryotyping of pediatric acute lymphoblastic leukemias by high-resolution single nucleotide polymorphism oligonucleotide genomic microarray. Blood. 2008;111:776-784.
22. Raghavan M, Lillington DM, Skoulakis S, et al. Genome-wide single nucleotide polymorphism analysis reveals frequent partial uniparental disomy due to somatic recombination in acute myeloid leukemias. Cancer Res. 2005;65:375-378.
23. Fitzgibbon J, Smith LL, Raghavan M, et al. Association between acquired uniparental disomy and homozygous gene mutation in acute myeloid leukemias. Cancer Res. 2005;65:9152-9154.
24. Serrano E, Carnicer MJ, Orantes V, et al. Uniparental disomy may be associated with microsatellite instability in acute myeloid leukemia (AML) with a normal karyotype. Leuk Lymphoma. 2008;49:1178-1183.
25. Gupta M, Raghavan M, Gale RE, et al. Novel regions of acquired uniparental disomy discovered in acute myeloid leukemia. Genes Chromosomes Cancer. 2008;47:729-739.
26. Raghavan M, Smith LL, Lillington DM, et al. Segmental uniparental disomy is a commonly acquired genetic event in relapsed acute myeloid leukemia. Blood. 2008;112:814-821.
27. Gorletta TA, Gasparini P, D'Elios MM, Trubia M, Pelicci PG, Di Fiore PP. Frequent loss of heterozygosity without loss of genetic material in acute myeloid leukemia with a normal karyotype. Genes Chromosomes Cancer. 2005;44:334-337.
28. Akagi T, Ogawa S, Dugas M, et al. Frequent genomic abnormalities in acute myeloid leukemia/myelodysplastic syndrome with normal karyotype. Haematologica. In press.
29. National Center for Biotechnology Information. Gene Expression Omnibus (GEO). http://www.ncbi.nlm.nih.gov/geo. Accessed December 2008.
30. Shih LY, Kuo MC, Liang DC, et al. Internal tandem duplication and Asp835 mutations of the FMS-like tyrosine kinase 3 (FLT3) gene in acute promyelocytic leukemia. Cancer. 2003;98:1206-1216.
31. The Centre for Applied Genomics. Database of Genomic Variants. http://projects.tcag.ca/variation. Accessed April 2008.
32. University of California Santa Cruz. UCSC Genome Browser. http://genome.ucsc.edu. Accessed May 2004.
33. Kelly LM, Liu Q, Kutok JL, Williams IR, Boulton

CL, Gilliland DG. FLT3 internal tandem duplication mutations associated with human acute myeloid leukemias induce myeloproliferative disease in a murine bone marrow transplant model. Blood. 2002;99:310-318.

34. Grundler R, Miething C, Thiede C, Peschel C, Duyster J. FLT3-ITD and tyrosine kinase domain mutants induce 2 distinct phenotypes in a murine bone marrow transplantation model. Blood. 2005; 105:4792-4799.
35. Choudhary C, Schwable J, Brandts C, et al. AML-associated Flt3 kinase domain mutations show signal transduction differences compared with Flt3 ITD mutations. Blood. 2005;106:265-273.
36. Kubonishi I, Machida K, Niiya K, et al. Establishment of a new peroxidase-positive human myeloid cell line, PL-21. Blood. 1984;63:254-259.
37. Lanotte M, Martin-Thouvenin V, Najman S, Balerini P, Valensi F, Berger R. NB4, a maturation inducible cell line with t(15;17) marker isolated from a human acute promyelocytic leukemia (M3). Blood. 1991;77:1080-1086.
38. Mozziconacci MJ, Rosenauer A, Restouin A, et al. Molecular cytogenetics of the acute promyelocytic leukemia-derived cell line NB4 and of four all-trans retinoic acid-resistant subclones. Genes Chromosomes Cancer. 2002;35:261-270.
39. Tickenbrock L, Schwäble J, Wiedehage M, et al. Flt3 tandem duplication mutations cooperate with Wnt signaling in leukemic signal transduction. Blood. 2005;105:3699-3706.
40. Li L, Piloto O, Kim KT, et al. FLT3/ITD expression increases expansion, survival and entry into cell cycle of human haematopoietic stem/progenitor cells. Br J Haematol. 2007;137:64-75.
41. Kim KT, Baird K, Davis S, et al. Constitutive Fms-like tyrosine kinase 3 activation results in specific changes in gene expression in myeloid leukaemic cells. Br J Haematol. 2007;138:603-615.
42. Hernandez JM, Gonzalez MB, Garcia JL, et al. Two cases of myeloid disorders and a t(8;12)(q12;p13). Haematologica. 2000;85:31-34.
43. Barjesteh van Waalwijk van Doorn-Khosrovani S, Spensberger D, de Knegt Y, Tang M, Löwenberg B, Delwel R. Somatic heterozygous mutations in ETV6 (TEL) and frequent absence of ETV6 protein in acute myeloid leukemia. Oncogene. 2005; 24:4129-4137.
44. Marcucci G, Baldus CD, Ruppert AS, et al. Overexpression of the ETS-related gene, ERG, predicts a worse outcome in acute myeloid leukemia with normal karyotype: a Cancer and Leukemia Group B study. J Clin Oncol. 2005; 23:9234-9242.

Frequent genomic abnormalities in acute myeloid leukemia/myelodysplastic syndrome with normal karyotype

Tadayuki Akagi,[1*] Seishi Ogawa,[2,3,4] Martin Dugas,[5] Norihiko Kawamata,[1] Go Yamamoto,[2] Yasuhito Nannya,[2] Masashi Sanada,[3,4] Carl W. Miller,[1] Amanda Yung,[1] Susanne Schnittger,[6] Torsten Haferlach,[6] Claudia Haferlach,[6] and H. Phillip Koeffler[1]

[1]Division of Hematology and Oncology, Cedars-Sinai Medical Center, UCLA School of Medicine, Los Angeles, CA, USA; [2]Department of Hematology and Oncology, and [3]Department of Cell Therapy and Transplantation Medicine and the 21st Century COE Program, Graduate School of Medicine, University of Tokyo, Tokyo, Japan; [4]Core Research for Evolutional Science and Technology, Japan Science and Technology Agency, Tokyo, Japan; [5]Department of Medical Informatics and Biomathematics, University of Munster, Munster, Germany; [6]MLL Munich Leukemia Laboratory, Munich, Germany

ABSTRACT

Background

Acute myeloid leukemia is a clonal hematopoietic malignant disease; about 45-50% of cases do not have detectable chromosomal abnormalities. Here, we identified hidden genomic alterations and novel disease-related regions in normal karyotype acute myeloid leukemia/myelodysplastic syndrome samples.

Design and Methods

Thirty-eight normal karyotype acute myeloid leukemia/myelodysplastic syndrome samples were analyzed with high-density single-nucleotide polymorphism microarray using a new algorithm: allele-specific copy-number analysis using anonymous references (AsCNAR). Expression of mRNA in these samples was determined by mRNA microarray analysis.

Results

Eighteen samples (49%) showed either one or more genomic abnormalities including duplication, deletion and copy-number neutral loss of heterozygosity. Importantly, 12 patients (32%) had copy-number neutral loss of heterozygosity, causing duplication of either mutant *FLT3* (2 cases), *JAK2* (1 case) or *AML1/RUNX1* (1 case); and each had loss of the normal allele. Nine patients (24%) had small copy-number changes (< 10 Mb) including deletions of *NF1*, *ETV6/TEL*, *CDKN2A* and *CDKN2B*. Interestingly, mRNA microarray analysis showed a relationship between chromosomal changes and mRNA expression levels: loss or gain of chromosomes led, respectively, to either a decrease or increase of mRNA expression of genes in the region.

Conclusions

This study suggests that at least one half of cases of normal karyotype acute myeloid leukemia/myelodysplastic syndrome have readily identifiable genomic abnormalities, as found by our analysis; the high frequency of copy-number neutral loss of heterozygosity is especially notable.

Key words: normal karyotype acute myeloid leukemia/myelodysplastic syndrome, SNP-chip, CNN-LOH.

Citation: Akagi T, Ogawa S, Dugas M, Kawamata N, Yamamoto G, Nannya Y, Sanada M, Miller CW, Yung A, Schnittger S, Haferlach T, Haferlach C, and Koeffler HP. Frequent genomic abnormalities in acute myeloid leukemia/myelodysplastic syndrome with normal karyotype. Haematologica 2009; Haematologica 2009; 94:213-223. doi:10.3324/haematol.13024

CH and HPK are co-last authors.

[*]Current address: Department of Stem Cell Biology, Graduate School of Medical Science, Kanazawa University. 13-1 Takara-machi, Kanazawa, Ishikawa 920-8640, Japan

Acknowledgments: we thank members of our laboratory for helpful discussions.

Funding: this work was supported by NIH grants as well as the Parker Hughes Fund. HPK is the holder of the Mark Goodson endowed Chair in Oncology Research and is a member of the Jonsson Cancer Center and the Molecular Biology Institute, UCLA. MD and TH are supported by the European Leukemia Network (funded by the 6th Framework Program of the European Community). The study is dedicated to the memory of David Golde, a mentor and friend.

Manuscript received March 5, 2008. Revised version arrived September 17, 2008. Manuscript accepted October 6, 2008.

Correspondence: Tadayuki Akagi, Ph.D, Division of Hematology and Oncology, Cedars-Sinai Medical Center, UCLA School of Medicine 8700 Beverly Blvd, Los Angeles, CA90048, USA. E-mail: tadayuki@staff.kanazawa-u.ac.jp

The online version of this article contains a supplementary appendix.

Introduction

Acute myeloid leukemia (AML) is a clonal malignant hematopoietic disease characterized by a block in differentiation, resulting in accumulation of immature myeloid cells.[1,2] Karyotypic analyses have revealed several frequent chromosomal translocations producing fusion genes associated with AML. The t(8;21)(q22;q22) translocation is one of these abnormal karyotypes, and this translocation produces *AML1-ETO* fusion products.[3,4] The *AML1-ETO* blocks hematopoietic differentiation and enhances self-renewal of human and murine hematopoietic stem cells.[5,6] The fusion product apparently binds to *AML1* target genes and represses their transcription.[5,6] The inv(16)(p13q22) or t(16;16)(p13;q22) produces the leukemogenic *CBFB-MYH11* fusion gene which blocks differentiation of hematopoietic stem cells by inhibiting the function of *AML1*.[7,8] Acute promyelocytic leukemia cells usually have t(15;17)(q22;q11-21) producing *PML-RARA* fusion products which also behave as a transcriptional repressor.[9,10] Other frequent translocations include t(9;11), t(6;11), inv(3)/t(3;3) and t(6;9).[11] Trisomy 8, 11, 13, 21 and 22, and deletion of chromosome 5/5q, 7/7q, 17/17p and 20/20q also occur moderately frequently.[2,11,12] About 45-50% of AML patients have no detectable chromosomal abnormalities.[13,14] In general, these individuals with a normal karyotype in their leukemic cells show an intermediate prognosis.[13,14]

Besides chromosomal abnormalities, the leukemic cells can have a variety of mutations involving individual genes. Activating mutations of the receptor tyrosine kinase, FMS-like tyrosine kinase 3 (*FLT3*) occur in about 30% AML patients; two major mutant forms occur: an internal tandem duplication (ITD) or a point mutation in the tyrosine kinase domain (TKD).[15] Activating mutations at codon 12, 13 or 61 of either the *NRAS* or *KRAS* occur in 25% and 15% of AML patients, respectively.[1,16] About 10-15% of AML samples have inactivating mutations of C/EBPα whose wild-type function is to enhance differentiation.[17,18] Nucleophosmin1 (NPM1) is mutated in 50-60% of AML samples with normal karyotype.[15,19] This protein has an important role in ribosome biogenesis, including nuclear export of ribosomal proteins. Mutant NPM1 has an aberrant nuclear export signal and remains localized in the cytoplasm.[20]

Single-nucleotide polymorphism microarray (SNP-chip) analysis is a new technique to examine the genome including any copy-number changes and loss of heterozygosity (LOH).[21-25] Importantly, SNP-chip analysis can reveal cryptic abnormalities such as a small copy-number changes (< 10 Mb) or copy-number neutral loss of heterozygosity [CNN-LOH, also called uniparental disomy (UPD)] that cannot be detected by karyotype analysis. In addition, comparative genomic hybridization cannot detect CNN-LOH. SNP-chip analysis has been used in chronic lymphocytic leukemia,[24,25] childhood acute lymphoblastic leukemia,[26,27] juvenile myelomonocytic leukemia,[28] follicular lymphoma,[29] multiple myeloma,[30] and AML.[31,32,50,51]

In the present study, we identified hidden abnormalities and novel disease-related genomic regions using 250 K SNP-chip analysis in samples from patients with normal karyotype AML/myelodysplastic syndrome (MDS). The use of CNAG (copy-number analysis for Affymetrix GeneChips) program[21] and a new algorithm AsCNAR (allele-specific copy-number analysis using anonymous references)[23] provided a highly sensitive technique to detect CNN-LOH, as well as, copy-number changes in AML/MDS genomes.

Design and Methods

Patients' samples

Samples from 30 anonymized patients with normal karyotype AML and 8 anonymized patients with normal karyotype MDS (age, 33-88 years; median, 62 years) were examined. These samples were isolated from bone marrow at diagnosis. The patients' age, gender, diagnosis, white blood cell count (WBC), karyotype and additional mutations of *FLT3* and *NPM1* are summarized in Table 1. This study was approved by Cedars-Sinai Medical Center (IRB number 4485).

High-density SNP-chip analysis

Genomic DNA was isolated from AML/MDS cells, and the DNA was subjected to GeneChip Human mapping 250 K array NspI microarray (SNP-chip, Affymetrix, Santa Clara, CA, USA) as described previously.[21,23] Hybridization, washing and signal detection were performed on GeneChip Fluidics Station 400 and GeneChip scanner 3000 according to the manufacturer's protocols (Affymetrix). Microarray data were analyzed for determination of both total and allelic-specific copy-number using the CNAG program as previously described[21,25] with minor modifications; the status of copy-numbers as well as CNN-LOH at each SNP was inferred using the algorithms based on hidden Markov models.[21,23] GNAGraph software was used for clustering of AML samples with regards to their copy-number changes, as well as CNN-LOH.[27] Size, position and location of genes were identified with UCSC Genome Browser *http://genome.ucsc.edu*. Copy-number changes, including duplication and deletion, were identified by allele-specific CNAG software.[23,27] These copy-number changes include copy-number variant and physiological deletion at the immunoglobulin and T-cell receptor genes. Copy-number variants as described previously at *http://projects.tcag.ca/variation* and physiological deletions were eliminated manually, and other regions detected by allele-specific CNAG software are listed on Table 4.

Fluorescence in situ hybridization analysis

Bone marrow samples from AML patients were used for interphase fluorescence *in situ* hybridization (FISH) analysis. The FISH studies were performed using the following probes: D5S721 (5p15.2), D5S23 (5p15.2), D7Z1 (centromere of chromosome 7), ABL (9q34.12), EGR1 (5q31.2), D7S486 (7q31), TP53 (17p13.1), D8Z2 (centromere of chromosome 8), AML1 (21q22.12) and BCR (22q11.23) (ABBOTT/VYSIS, Des Plaines, IL, USA). Probes for the 12p13 region [fluorescein-labeled ETV6-

downstream region (483 kb-length) and Texas-red-labeled ETV6-upstream region (264 kb-length)] were used for FISH analysis in case #5. The ETV6 probes were obtained from ABBOTT/VYSIS.

Determination of SNP sequences, JAK2, FLT3, NPM1, and AML1/RUNX1 mutations, and other target genes in cases of CNN-LOH

To determine the SNP sequences, (SNP identities are rs7747259, rs1122637, rs9505293, rs6934027, rs280153 and rs191986) in case #38 chromosome 6p region, the genomic region of each SNP site was amplified by genomic polymerase chain reaction (PCR) using specific primers. For determination of *JAK2* V617F mutation in case #20, genomic PCR was performed with specific primers. PCR products were purified and sequenced. The sequences of the primers are shown in *Online Supplementary Tables S1 and S2*. To determine the *FLT3*-ITD mutation, the PCR reaction was performed with specific primers, and the PCR products were separated on a 2.0% agarose gel stained with ethidium bromide as described previously[34,35] Mutations at exon 12 of the *NPM1* gene were determined using a melting curve-based LightCycler assay (Roche Diagnostics, Mannheim, Germany).[36] Denaturing high-performance liquid chromatography analysis was performed to determine the *AML1/RUNX1* mutation in case #17 as described previously.[37] Alterations of several tyrosine kinase genes including *FGR* (case #3 and #23), *DDR1* (case #2 and 38), *TYK2* (case #2), *MATK* (case #2), *FER* (case #8) and *FGFR4* (case #8) were determined by either nucleotide sequencing of their exons and/or band-shifts of PCR products of exons after their electrophoresis and visualization on a gel (single strand conformation polymorphism), as described previously[32] with minor modifications. The PCR reaction contained genomic DNA, 500 nM of each of the primers, 200 nM of each of the dNTP, 0.5 units of Taq DNA polymerase and 3 μCi [α-32P] dCTP in 20 μL PCR products were diluted 10-fold in the loading buffer (10 mM NaOH, 95% formamide, and 0.05% of both bromophenol blue and xylene cyanol). After denaturation at 94°C for 5 min, 2 mL of the samples were loaded onto a 6% non-denaturating polyacrylamide mutation detection enhancement gel (Bioproducts, Rockland, ME, USA) with 10% (v/v) glycerol and separated at 300 V for 20 h. The gel was dried and subjected to autoradiography.

Table 1. **Baseline clinical characteristics of 38 cases of normal karyotype acute myeloid leukemia/myelodysplastic syndrome.**

Group	Case #	Gender	Age	Type	WBC (×10⁹/L)	FLT3	NPM1	Karyotype
A	29	M	49	AML M0	13.8	–	–	46,XY
	1	F	33	AML M1	3.5	–	–	46,XX
	14	M	43	AML M1	27.9	–	–	46,XY
	15	F	67	AML M1	365	–	+	46,XX
	6	M	66	AML M2	2.5	–	–	46,XY
	24	M	88	AML M2	6.3	–	–	46,XY
	25	F	61	AML M2	11.9	–	+	46,XX
	33	F	60	AML M2	24.5	+	+	46,XX
	44	M	65	AML M2	62.8	–	–	46,XY
	18	F	43	AML M4	43.1	–	+	46,XX
	19	M	37	AML M4	209	–	+	46,XY
	32	M	45	AML M4	9.5	–	+	46,XY
	34	F	80	AML M4	71.1	+	–	46,XX
	31	F	45	AML M5b	12.7	+	+	46,XX
	16	F	77	MDS RA	5.3	–	–	46,XX
	35	F	68	MDS CMML-1	5.6	–	–	46,XX
	36	F	69	MDS RAEB-1	4.6	–	–	46,XX
	39	F	74	MDS RAEB-1[1]	5.4	–	–	46,XX
	42	F	79	MDS	3.2	–	–	46,XX
B	10	F	49	AML M1	17.0	+	–	46,XX
	4	M	76	AML M2	2.3	–	–	46,XY
	5	F	67	AML M2	1.1	–	–	46,XX
	8	F	75	AML M2	1.8	–	–	46,XX
	9	M	65	AML M2	48.3	–	–	46,XY
	17	M	78	AML M2	1.1	–	–	46,XY
	20	F	65	AML M2	34.3	–	–	46,XX
	23	M	69	AML M2	2.0	–	+	46,XY
	26	M	36	AML M2	14.2	–	+	46,XY
	2	F	71	AML M4	1.9	–	+	46,XX
	7	F	85	AML M4	2.4	–	–	46,XX
	21	F	38	AML M4	37.6	+	+	46,XX
	38	M	53	AML M4	40	+	+	46,XY
	3	F	67	AML M5b	56	+	+	46,XX
	37	F	65	AML M5b	72.8	+	+	46,XX
	12	M	69	MDS RA	11.5	–	–	46,XY
	41	M	77	MDS RA[1]	7.1	–	–	46,XY
	13	F	54	MDS RAEB-2	–	–	–	46,XX
	11	F	60	t-AML M2	1.7	–	–	46,XX

t-AML: therapy-related AML; RA: refractory anemia; RAEB-1 or -2: refractory anemia with excess blasts subtype-1 or -2; CMML: chronic myelomonocytic leukemia; [1]new WHO classification.

Quantitative real-time polymerase chain reaction

Gene-dosages of chromosome 6p24.3 in case #38, and the *MYC* and *CDKN2A* genes in case #20 were determined by quantitative real-time PCR (iCycler, Bio-Rad, Hercules, CA, USA) using Sybr Green. To determine the relative gene dosage of each sample, the chromosome 2p21 region was measured as a control.[27] The copy-number of the 2p21 region was normal, as determined by SNP-chip analysis, in these samples. The delta threshold cycle value (ΔCt) was calculated from the given Ct value by the formula ΔCt = (Ct sample - Ct control). The fold change was calculated as $2^{-\Delta Ct}$. Primer sequences are shown in *Online Supplementary Table S2*.

Gene expression microarray analysis

Total RNA was isolated from AML/MDS cells and processed according to Affymetrix guidelines for analysis with HGU133 Plus 2.0 microarrays. Data were analyzed with R version 2.5.0 using Bioconductor version 2.0.[40] Data were normalized using the robust multi-array average procedure.[39] Since most regions that showed chromosomal abnormalities were not recurring, we were not able to compare individual genes across samples with statistical tests. To assess plausibility of large deletions and amplifications, we subtracted

from each gene (in the respective region) mean expression of this gene in other cases: case #11 was compared with 37 normal karyotype AML/MDS cases; and cases #20, #4 and #5 were compared with other normal karyotype AML/MDS samples. We then calculated a mean expression difference for each region and considered a value below zero to be consistent with deletion and a value above zero to be consistent with amplification.

Results

Proof of principal

To identify hidden abnormalities in AML/MDS with a normal karyotype, 37 samples were analyzed by 250K SNP-chip microarray. One additional case (case #11) had only 13 metaphases and chromosomal abnormalities were not detected on karyotypic analysis; this sample did, however, have numerous genetic abnormalities identified by SNP-chip including hemizygous deletions of 3p25.1-p24.3 (2.29 Mb), 3p24.2-p24.1 (3.96 Mb), 3p23-q12.1 (66.55 Mb), 5q11.2-q-terminal (124.89 Mb), 7q11.23-q36.1 (76.04 Mb), 7q36.2 (0.78 Mb), 11q23.3-q-terminal (18.24 Mb), 17p-terminal-q11.1 (22.48 Mb), and 17q11.2-q12 (4.42 Mb); duplications of 3p24.3 (2.14 Mb), 5p15.31 (1.83 Mb), and 5p14.3-q11.2 (35.53 Mb); and trisomy of chromosomes 8, 21 and 22 (Table 2). To confirm these SNP-chip results, we performed extensive FISH analysis. The number of signals for probes D5S721 (5p15.2), D5S23 (5p15.2), D7Z1 (centromere of chromosome 7) and ABL (9q34.12) was two, and SNP-chip analysis also showed normal copy number (2n) consistent with the SNP-chip data. The EGR1 (5q31.2), D7S486 (7q31) and TP53 (17p13.1) probes revealed one signal; and these regions also showed hemizygous deletion (1n) by SNP-chip analysis. D8Z2 (centromere of chromosome 8), AML1 (21q22.12) and BCR (22q11.23) probes showed three or four signals, and SNP-chip analysis also indicated trisomy (3n) of these chromosomes. Chromosome 9 was normal by both SNP-chip and FISH analyses. As summarized in *Online Supplementary Table S3*, the results of SNP-chip and FISH analyses were completely congruent. Taken together, these results suggest that SNP-chip analysis reflected the genomic changes.

SNP-chip analysis in 37 normal karyotype acute myeloid leukemia/myelodysplastic syndrome samples

SNP-chip analysis of samples from 37 patients with normal karyotype AML/MDS revealed several genomic copy-number changes, as well as CNN-LOH. Nineteen patients (51%) had a normal genome by SNP-chip analysis (group A). In contrast, 18 patients (49%) had one or more genomic abnormalities (group B) (Figure 1). Deletions and/or duplications were found in nine patients (24%). Twelve patients (32%) had CNN-LOH. In group B, 14 cases (78% of the 18 samples) had only one genomic change; one case (6%) had two genomic abnormalities (case #5); two cases (11%) had three changes (case #2 and #4) and one case (5%) had four genomic alterations (case #20).

We also compared the relationship between the genomic changes and the French-American British classification of the 15 AML and 3 MDS samples in group B. In the AML samples, 11 cases had CNN-LOH, three cases had a duplication and seven cases had a deletion. The one AML M1 sample (case #10) had CNN-LOH; and the two AML M5b samples (cases #3 and #37) had CNN-LOH in their chromosomes. In the four AML M4 samples, cases #38, #21 and #2 had CNN-LOH, and cases #2 and #7 had a small deletion. In eight AML M2 samples, five (cases #4, #8, #17, #20, and #23) had CNN-LOH, three (cases #4, #5 and #20) had a duplication, and five (cases # 4, #5, #9, #20 and #26) had a deletion. In the three MDS samples, one sample (case #12) had CNN-LOH, and two samples (cases #13 and #41) had a deletion (Figure 1, Tables 3 and 4). Taken together, these results show that the patients who were categorized as having normal karyotype AML/MDS had easily recognizable deletions, duplications and/or CNN-LOH of their genome.

Table 2. **Copy-number changes in case #11 detected by SNP-chip analysis.**

Chromosome	Location	Physical location		Size (Mb)	Status
		Proximal	Distal		
3	3p25.1-p24.3	16,389,202	18,675,075	2.29	Del
	3p24.3	19,589,378	21,731,557	2.14	Dup
	3p24.2-p24.1	24,881,910	28,844,599	3.96	Del
	3p23-q12.1	33,278,003	99,828,897	66.55	Del
5	5p15.31	7,616,335	9,443,217	1.83	Dup
	5p14.3-q11.2	18,603,838	54,129,781	35.53	Dup
	5q11.2-q-ter.	55,738,905	180,629,495	124.89	Del
7	7q11.23-q36.1	71,659,926	147,695,696	76.04	Del
	7q36.2	152,027,450	152,806,031	0.78	Del
8	Trisomy				
11	11q23.3-q-ter.	116,202,097	134,439,182	18.24	Del
17	17p-ter.-q11.1	18,901	22,494,871	22.48	Del
	17q11.2-q12	25,499,505	29,918,396	4.42	Del
21	Trisomy				
22	Trisomy				

AML case #11 had numerous genetic abnormalities. Location and size (Mb) were obtained from UCSC Genome Browser. Copy-number changes previously described as copy-number variant were excluded. Del: deletion; Dup: duplication; ter: terminal.

Chromosomal region and candidate genes in CNN-LOH detected by SNP-chip analysis

Previous studies demonstrated CNN-LOH in AML samples at a frequency of 15-20%.[31,32,50,51,53,54] Our analysis with AsCNAR (allele-specific copy-number analysis using anonymous references) revealed CNN-LOH in 32% of the AML/MDS samples with a normal karyotype; the median size of the CNN-LOH was 30.91 Mb (range, 11.76 Mb–103.77 Mb). We found some cases with a recurrent region of CNN-LOH. Cases #3 and #23 had CNN-LOH on 1p, and the common region of CNN-LOH (30.85 Mb) included the tyrosine kinase genes (*FGR*, *EPHA2* and *EPHB2*) and an imprinted tumor suppressor gene *TP73* (Table 3). Cases #2 and #38 had CNN-LOH on 6p and the common region of CNN-LOH (30.97 Mb) contained the tyrosine kinase gene *DDR1* (Table 3). Cases #4 and #37 had CNN-LOH on 8q and the common region of CNN-LOH (11.76 Mb) contained the tyrosine kinase gene *PTK* (Table 3). CNN-LOH of the

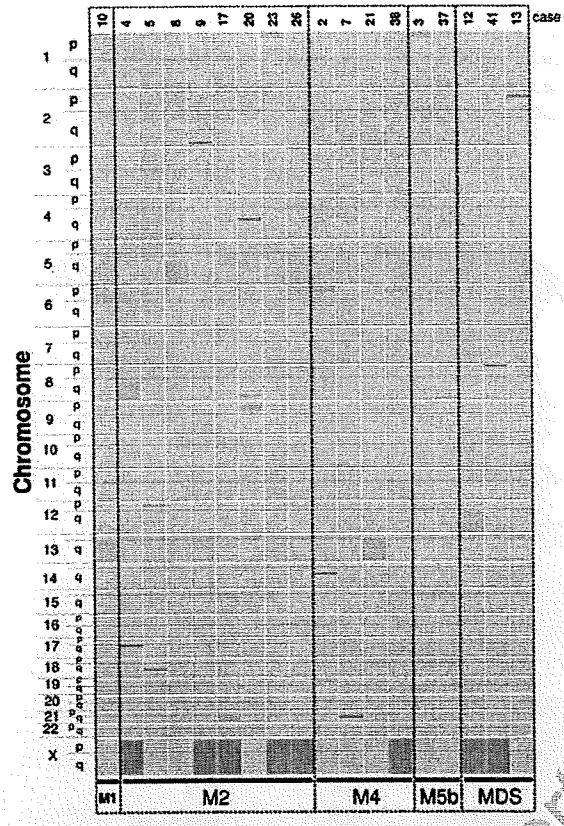

Figure 1. Genomic DNA of 37 acute myeloid leukemia samples with normal karyotype were subjected to SNP-chip analysis; genomic abnormalities are summarized. Pink, green and red bars/boxes indicate CNN-LOH, deletion and duplication, respectively. Nineteen patients (51%) showed no detectable genomic abnormalities (*data not shown*), whereas 18 patients (49%) had one or more genomic abnormalities. Deletion or duplication was found in nine patients (24%), and CNN-LOH occurred in 12 patients (32%). Chromosomal location, size and genes are shown in Tables 3 and 4.

whole region of 13q was found in cases #10 and #21; this region contains the *FLT3*, *FLT1*, *BRCA2* and *RB1* genes (Table 3).

Cases #2, #8, #12, #17 and #20 had CNN-LOH on 19p (13.41 Mb), 5q (103.77 Mb), 12q (96.23 Mb), 21q (29.54 Mb) and 9p (43.96 Mb), respectively. Although these regions of CNN-LOH occurred in only one case each, several interesting genes were found in the region, including *INSR*, *TYK2*, and *MATK* (case #2); *APC*, *FER*, *FMS/FLT4*, *PDGFRB*, *ITK* and *FGFR4* (case #8), *AML1/RUNX1* (case #17), and *JAK2* and *TEK* (case #20) (Table 3).

Interestingly, cases #10 and #21 had a *FLT3*-ITD gene mutation (Table 3); case #17 had an *AML1/RUNX1* frameshift caused by a deletion of cytosine at nucleotide 211 (Table 3). Sequencing of *JAK2* in case #20 showed a homozygous canonical *JAK2* mutation [V617F (GTC → TTC)] (Table 3). Each of these mutations occurred at a CNN-LOH. The data suggest that removal of a normal allele and duplication of the mutated allele is favored by the cancer cells.

Validation of copy number-neutral loss of heterozygosity

To validate CNN-LOH, we determined SNP sequences and gene-dosage in a CNN-LOH region using case #38 (Figure 2). If a chromosome has LOH, the nucleotide at the SNP site should not be heterozygous, but should be homozygous. We, therefore, examined six independent SNP sites in case #38 on the chromosome 6p region of CNN-LOH including rs7747259, rs1122637, rs9505293, rs6934027, rs280153 and rs191986. All six SNP sites showed only a single nucleotide; no SNP sites showed heterozygosity (Figure 2B). Each one of these sites is heterozygous in the general population at a frequency varying between 25% and 42% (*Entrez SNP database, http://www.ncbi.nlm.nih.gov/sites/entrez?db=snp*). These results strongly suggest that this region has LOH.

Next, we determined gene-dosage of the region to exclude the possibility of hemizygous deletion. The gene-dosage of 6p24.3 in case #38 was compared to that of normal genomic DNA using quantitative genomic real-time PCR by comparing the ratio between 6p24.3 and the reference genomic DNA, 2p21. As shown in Figure 2C, the amount of DNA at this site for case #38 was almost the same as that for normal genomic DNA, indicating that this region is not deleted. Taken together, our sequence data and gene dosage study validated the results of our SNP-chip analysis, clearly showing CNN-LOH at 6p24.3.

Chromosomal regions of copy-number change detected by SNP-chip analysis

Nine patients (24%) had small copy-number changes including deletions and/or duplications; the median size of the duplications and deletions was 0.3 Mb (range, 0.09–4.33 Mb) and 0.625 Mb (range, 0.11–5.87 Mb), respectively. As shown in Table 4, hemizygous deletions were found at 14q21.2 (0.3 Mb, case #2), 17q11.2 (2.7 Mb, case #4), 12p13.31 - p13.2 (2.91 Mb, case #5), 21q21.2 (0.44 Mb, case #7), 2q36.2 (0.41 Mb, case #9), 2p23.1 (0.56 Mb, case #13), 4q24 (1.08 Mb, case #20), 9p21.3 - p21.2 (5.87 Mb, case #20), 3p26.3 (0.69 Mb, case #26), and 8p23.2 (0.11 Mb, case #41). Cases #4, #5 and #20 had duplication at 1q43 (0.09 Mb), 18q21.2 (0.3 Mb), and 8q24.13 - q24.21 (4.33 Mb), respectively. These regions contain well-known oncogenes and tumor suppressor genes (Table 4). The tumor suppressor genes, *NF1* and *CDKN2A/CDKN2B*, and the transcription factor, *ETV6/TEL* were deleted in cases #4, #20 and #5, respectively; and the oncogene *MYC* was duplicated in case #20.

Validation of copy-number changes

Next, we validated copy-number changes in cases #20 and #5 using different techniques. Case #20 had duplication at 8q24.13 - q24.21 (Figure 3A) and hemizygous deletion at 9p21.3 - p21.2 (Figure 3B); these regions contain the oncogene *MYC* and the tumor suppressor genes *CDKN2A* and *CDKN2B*, respectively. Relative gene-dosages of the *MYC* and *CDKN2A* genes were examined by quantitative genomic real-time PCR with the chromosome 2p21 region as a control. The

level of the *MYC* gene was about 2-fold higher while the level of the *CDKN2A* gene was approximately 10-fold lower compared with normal genomic DNA (Figures 3C and D).

Chromosome 12p13.31 - p13.2 was deleted in case #5; this region contains the transcription factor *ETV6/TEL* (Figure 3E). FISH analysis with a probe of fluorescein-labeled ETV6-downstream (normal copy-number region) revealed two signals and a probe of Texas-red-labeled ETV6-upstream (hemizygous deleted region) revealed one signal (Figure 3F), validating the observations from SNP-chip analysis.

Table 3. **Chromosomal regions identified as CNN-LOH.**

Case	FAB	Location	Physical localization Proximal	Distal	Size (Mb)	Genes
3	AML M5b	1p-ter.-p35.2	825,852	31,679,683	30.85	*FGR*
23	AML M2	1p-ter.-p35.1	825,852	33,526,200	32.7	*EPHA2, EPHB2 EPHA8, TP73 LCK* (only #23)
2	AML M4	6p-ter. - p21.3	3119,769	31,094,483	30.97	*DDR1*
38	AML M4	6p-ter. - p21.3	1119,769	33,781,344	33.66	
4	AML M2	8q12.3 - q-ter.	64,069,382	146,106,670	82.04	*PTK2*
37	AML M5b	8q24.22 - q-ter.	134,507,898	146,263,538	11.76	*NBS1* (only #4)
10	AML M1	Whole 13q				*FLT3* (ITD)
21	AML M4	Whole 13q				*FLT1 BRCA2 RB1*
2	AML M4	19p-ter. - p13.13	212,033	13,625,099	13.41	*INSR, TYK2, MATK*
8	AML M2	5q13.3 - q-ter	76,761,338	180,536,297	103.77	*APC, FER, FMS/FLT4 PDGFRB, ITK, FGFR4, NPM1*
12	MDS RA	12q11 - q-ter.	36,144,018	132,377,151	96.23	*HER3*
17	AML M2	21q21.1 - q-ter.	17,346,621	46,885,639	29.54	*AML1/RUNX1* (delC211, frameshift)
20	AML M2	9p-ter. - p21.3 9p21.2 - q21.11	140,524 27,142,682	21,047,062 44,108,554	20.91 16.97	*JAK2* (V617F) *TEK*

*Twelve patients (32%) had CNN-LOH. Physical localization, size (Mb), and genes were obtained from UCSC Genome Browser. Note: Cases #10 and #21 had a mutant form of FLT3-internal tandem repeat [FLT3 (ITD)]. Case #20 had a mutant JAK2 (JAK2 V617F) which is constitutively active, and case #17 had a deletion of cytosine at nucleotide 211 of AML1/RUNX1, resulting in a frameshift. *, Known tyrosine kinase and tumor suppressor genes are shown.*

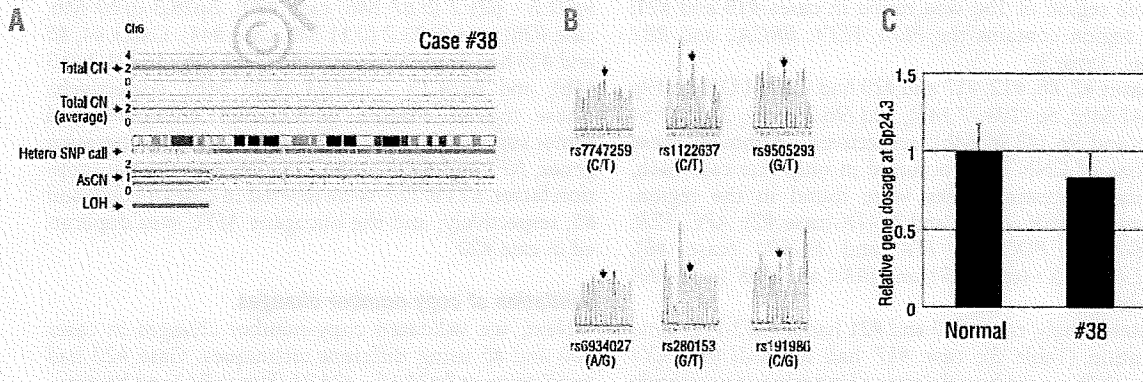

Figure 2. **Validation of CNN-LOH (A) Region of CNN-LOH in chromosome 6 of case #38. Red dots represent SNP sites as probes and indicate total copy-number. The blue line represents an average of copy-number and shows gene dosage. Green bars represents heterozygous (hetero) SNP calls. Red and green lines show allele-specific copy-number (AsCN). Blue bars indicate LOH detected by heterozygous SNP calls. (B) Determination of SNP sequences in the 6p region. Six independent SNP sites were sequenced. All six SNP sites contained only a single nucleotide; no SNP site displayed heterozygosity. Results are consistent with CNN-LOH. (C) Determination of gene-dosage in the 6p region. Gene-dosage of 6p24.3 (CNN-LOH region) in case #38 is compared to that in normal genomic DNA using quantitative genomic real-time PCR. Levels of the gene-dosage were determined as a ratio between 6p24.3 and the reference genomic DNA, 2p21.**

Table 4. **Chromosomal location of small copy-number changes.**

Case#	Type	Location	Physical localization (bp) Proximal	Distal	Size (Mb)	Status	Gene
4	AML M2	1q43	235,009,590	235,101,866	0.09	Dup	
		17q11.2	25,002,820	27,705,467	2.7	Del	*NF1*
5	AML M2	12p13.31-p13.2	9,312,096	12,218,922	2.91	Del	*ETV6/TEL*
		18q21.2	49,053,520	49,357,887	0.3	Dup	
9	AML M2	2q36.2	225,014,233	225,424,075	0.41	Del	
20	AML M2	4q24	105,640,274	106,723,813	1.08	Del	
		8q24.13 - q24.21	126,445,881	130,777,342	4.33	Dup	*MYC*
		9p21.3 - p21.2	21,063,692	26,935,976	5.87	Del	*CDKN2A, CDKN2B*
26	AML M2	3p26.3	1,221,075	1,911,873	0.69	Del	
2	AML M4	14q21.2	45,915,366	46,216,073	0.3	Del	
7	AML M4	21q21.2	23,126,095	23,566,855	0.44	Del	
41	MDS RA*	8p23.2	3,483,631	3,589,278	0.11	Del	
13	MDS RAEB-2	2p23.1	30,659,972	31,220,245	0.56	Del	

*Nine patients (24%) had deletion and/or duplication. Location, size (Mb), and genes were obtained from UCSC Genome Browser. Copy-number changes previously described as copy-number variant were excluded. Del; deletion, Dup; duplication. *Known oncogenes and tumor suppressor genes are shown.*

Relationship between genomic abnormalities and mutant genes within the region

In our normal karyotype AML/MDS samples, eight cases (21%) had *FLT3*-ITD and 14 cases (37%) had a *NPM1* mutation (Table 1). We compared genomic abnormalities, and *FLT3*-ITD and *NPM1* mutations (*Online Supplementary Table S4*). Both *FLT3*-ITD and *NPM1* were mutated in two samples in group A (11%) and four cases in group B (22%). A single mutation of *FLT3*-ITD was found in one sample in group A (5%) and one case in group B (6%); a single mutation of *NPM1* occurred in five samples in group A (26%) and three samples in group B (17%). These mutations were, therefore, dispersed between both groups A and B.

Relationship between genomic abnormalities and gene expression

We compared genomic abnormalities and gene expression. mRNA microarray analysis was done on all samples.[40] First, the level of mRNA expression in case #11 was compared with that in 37 normal karyotype AML samples. Affymetrix microarray analysis showed decreased average gene expression in the deleted regions and increased gene expression for regions with trisomy: the difference of average expression of genes located on deleted regions of chromosomes 5, 7, 17, as well as, trisomy 8, 21 and 22 were -0.21±0.01, -0.16 ±0.013, -0.27±0.018, +0.21±0.012, +0.22±0.022 and +0.15±0.013 (mean difference ± standard error), respectively (Figure 4A and *data not shown*).

Next, we examined the relationship between small copy-number changes and mRNA expression levels in the region. For this analysis, we chose deleted regions on chromosome 9 in case #20 (Figure 3B), chromosome 17 in case #4 (Table 4) and chromosome 12 in case #5 (Figure 3E). The differences in mean expression of genes located in deleted regions of chromosomes 9 (case #20), 17 (case #4), and 12 (case #5) were -0.15±0.07, -0.37±0.07, and -0.23±0.051 (mean difference ± standard error), respectively (Figure 4B). These results showed that large and small copy-number changes led to alterations of mRNA expression. In addition, the difference in mean expression of genes located in the CNN-LOH regions of each sample was comparable to that in normal copy-number samples, suggesting that CNN-LOH does not contribute to aberrant levels of gene expression (*data not shown*).

Discussion

Our genome-wide SNP-chip analysis of normal karyotype AML/MDS showed that 49% of these samples had one or more genomic abnormalities including deletions, duplications and CNN-LOH. Previous studies demonstrated that CNN-LOH occurs in AML samples at a frequency of 15-20%.[31,32,50,51,53,54] Of interest, about 40% of cases of relapsed of AML had CNN-LOH.[52] In our analysis, 32% of samples had CNN-LOH, and these regions of CNN-LOH contain several tyrosine kinase and tumor suppressor genes that may be candidate target genes in normal karyotype AML/MDS. In fact, the *FLT3*-ITD (13q12.2), *JAK2* V617F (9p24.1) and deletion of a cytosine at nucleotide 211 of *AML1/RUNX1* (21q22.12) occurred in areas of CNN-LOH resulting in duplication of these mutant genes and loss of the normal allele. A prior paradigm was that CNN-LOH marked the location of a mutated tumor suppressor gene, but it is clear that CNN-LOH can also be a signpost of an activated (mutated) oncogene. Of note, several CNN-LOH, including a region on chromosome 1p (cases #3 and #23), 6p (cases #2 and #38), 8q (cases #4 and 37) and 13q (cases #10 and #21), occurred in more than one sample. In addition, CNN-LOH of these regions, as well as several other unique CNN-LOH regions in our cohort, were also found in other stud-

ies.[30,31,55] Although these alterations are not frequent, shared regions of CNN-LOH clearly highlight their importance. These findings prompted us to screen genes located in CNN-LOH regions. We focused on tyrosine kinase genes including *FGR* (cases #3 and #23), *DDR1* (cases #2 and #38), *TYK2* (case #2), *MATK* (case #2), *FER* (case #8) and *FGFR4* (case #8), and either determined their exon nucleotide sequences or looked for single strand conformation polymorphism band-shifts of PCR products of the exons. However, these genes did not have detectable mutations (*data not shown*). Nevertheless, we believe that these CNN-LOH, as well as deletions and duplications, are acquired somatic mutations. We examined these regions for known copy-number polymorphisms (web site, *http://projects.tcag.ca/variation*) and found none. Also previously, we compared SNP-chip data between matched samples of acute promyelocytic leukemia and normal genomic DNA from the same individual (Akagi *et al.*, unpublished data) and found that CNN-LOH occurred only in the leukemia samples but not in the corresponding germline DNA. Furthermore, SNP-chip analysis easily detected a deletion on chromosome 3 (0.69 Mb) in case #28 in the AML sample which was not present in the remission bone marrow sample from the same individual (*Online Supplementary Figure S1*). Taken together, these findings suggest that the alterations detected by SNP-chip analysis are somatic mutations.

We also found small copy-number changes in some cases. Several features of case #20 are worthy of comment. The *MYC* gene was duplicated, and the *CDKN2A* (*p16/INK4A* and *p14/ARF*) and *CDKN2B* (*p15/INK4B*) genes were hemizygously deleted. Prominent expression of C-MYC protein is associated with stimulation of p14/ARF which inactivates MDM2, producing greater levels of p53 resulting in either apoptosis or slowing of cell growth which allows for DNA repair.[41,42] However, when the *p14/ARF* gene is deleted, C-MYC has an unfettered ability to stimulate growth of the cells. Case #20 had this constellation of changes. Furthermore, this individual had a homozygous *JAK2* mutation. *JAK2* is mutated (codon 617, valine changed to phenylalanine) and constitutively active in nearly 100%, 50% and 30% of samples from patients with polycythemia vera, agnogenic myeloid metaplasia and essential thrombocythemia, respectively, as well as in 1-3% of AML cases.[43-45] We do not know the prior history of this individual.

Some of the deleted genes are of particular interest; first, the tumor suppressor gene *NF1* was deleted in case #4. Children with neurofibromatosis type-1 have inactivating mutations of the *NF1* and an increased risk of developing juvenile myelomonocytic leukemia,[46] and LOH at the *NF1* gene locus occurs in this form of leukemia and other cancers. A recent study showed that three of 103 T-ALL (3%) samples and two of 71 AML samples with *MLL* rearrangements (3%) had deletion of the *NF1* gene region; a mutation in the remaining *NF1* allele was found in three samples, suggesting that *NF1* inactivation might be involved in the development of leukemia. Second, concerning case #5 (deletion of *ETV6/TEL*), *ETV6/TEL* is a transcriptional repressor and is involved in various translocations associated with

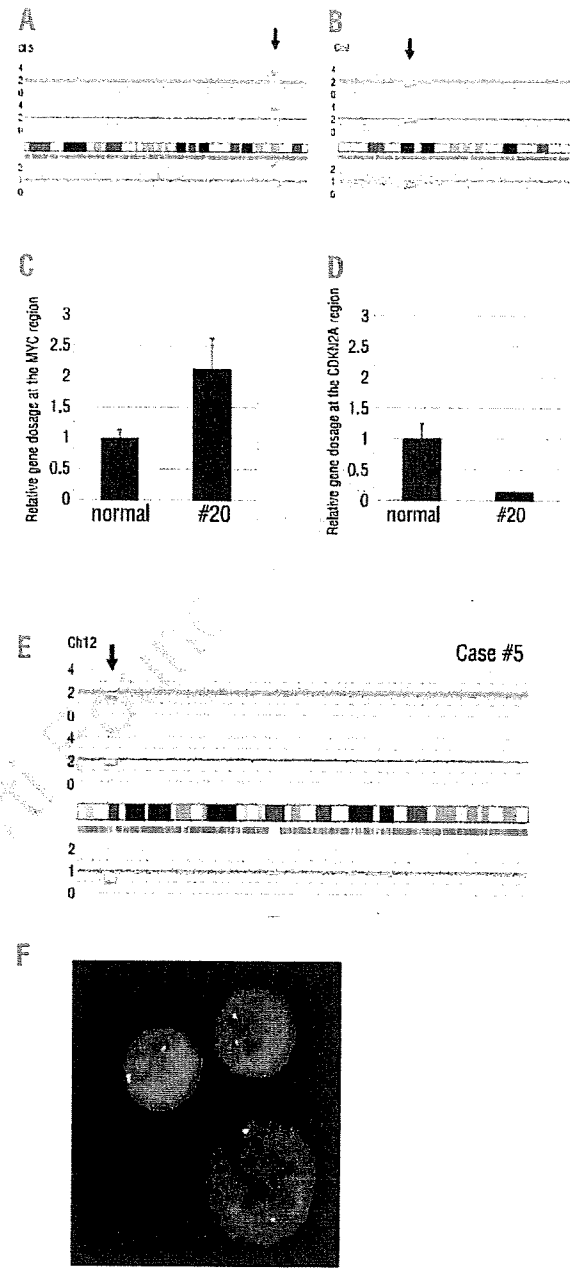

Figure 3. Validation of duplication and deletion: (A) Chromosome 8q24.13-q24.21 is duplicated. This region contains the oncogene *MYC*. (B) Chromosome 9p21.3 - p21.2 shows a deletion. The deleted region contains the tumor suppressor genes *CDKN2A* (*p16/INK4A* and *p14/ARF*) and *CDKN2B* (*p15/INK4B*). (C, D) Gene-dosages of the *MYC* gene (C) and the *CDKN2A* gene (D) region in case #20 are compared to normal genomic DNA by quantitative genomic real-time PCR. Levels of the gene-dosage are determined as a ratio between target gene and the reference genomic DNA, 2p21. (E) Case #5 had hemizygous deletion in chromosome 12p13.31-p13.2; this region contains the transcription factor *ETV6/TEL* gene. Physical localization and size are presented in Table 4. (F) FISH analysis of case #5 with probes for the *ETV6/TEL* region. Probes of fluorescein-labeled ETV6-downstream (normal region by SNP-chip analysis) and Texas-red-labeled ETV6-upstream (hemizygous deleted region by SNP-chip analysis) revealed one and two signals, respectively.

leukemia. About 30% of AML patients have loss of expression of the ETV6/TEL protein;[47,48] mutations of *ETV6/TEL* were found in 2% of AML samples, and these mutants behaved in a dominant-negative fashion.[48] Interestingly, previous array-comparative genome hybridization analysis of normal karyotype AML showed duplication of 8q24.13-q24.21 (including the *MYC* gene) and deletion of 12p12.3 (including the *ETV6* gene);[35] this constellation of alterations was also observed in our study.

Our microarray analysis showed that regions with copy-number loss or gain of chromosomal material

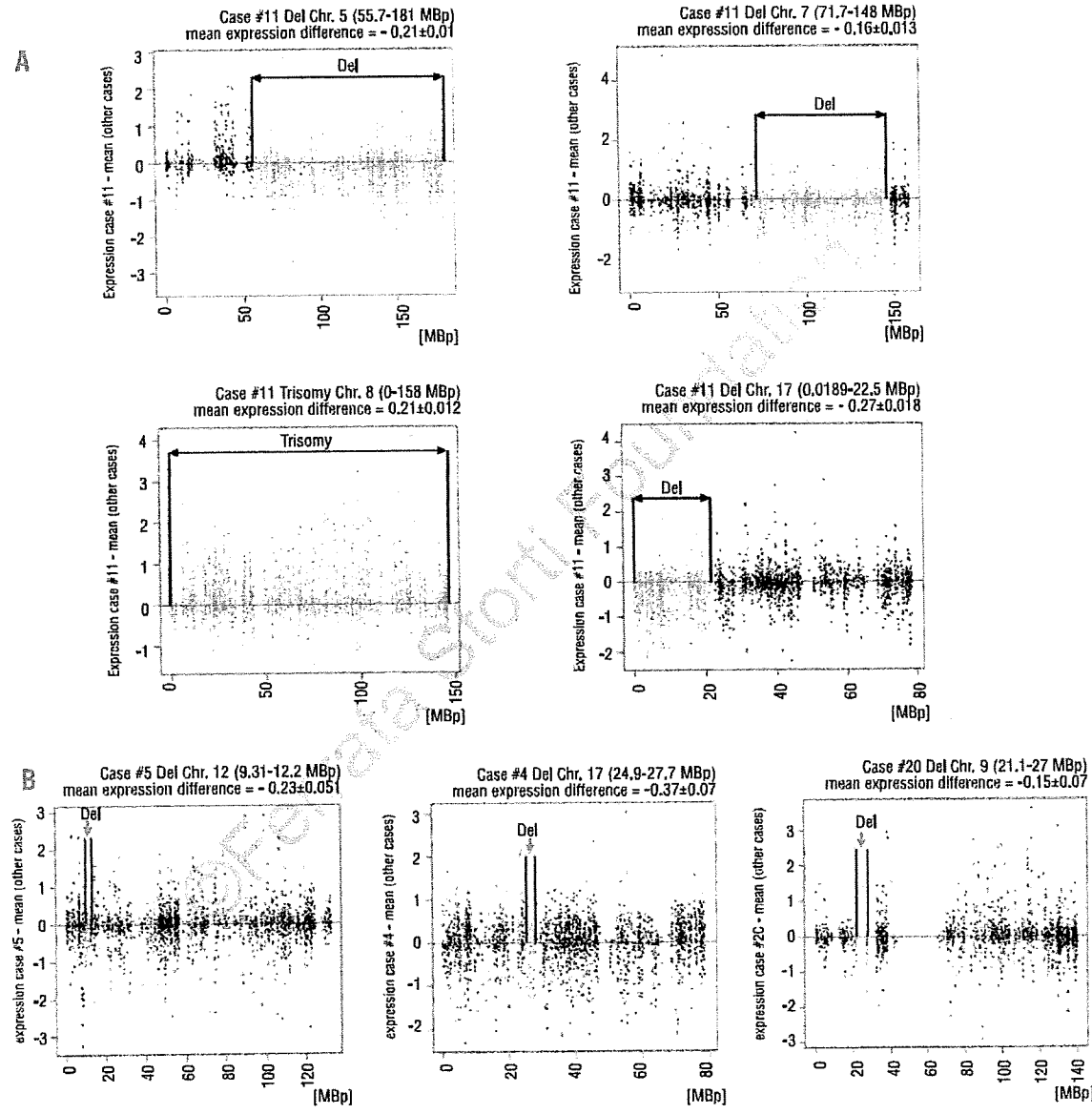

Figure 4. mRNA microarray analyses of acute myeloid leukemia samples. (A) Relationship between genomic abnormality and gene expression in acute myeloid leukemia case #11. mRNA microarray analysis was performed on all samples, and expression levels of acute myeloid leukemia cells from case #11 were compared to those of 37 normal karyotype acute myeloid leukemia samples. Affymetrix microarray analysis showed decreased average gene expression in the deleted regions, and increased average gene expression for trisomy 8: the difference of mean expression of genes located in the deleted region of chromosomes 5 (upper, left), 7 (upper, right), 17 (lower, right) and trisomy 8 (lower, left) were -0.21±0.01, -0.16±0.013, -0.27±0.018, and +0.21±0.012 (mean difference ± standard error), respectively. (B) Expression levels in acute myeloid leukemia cells from cases #20, #4 and #5 were compared with those in 36 normal karyotype AML samples. The differences in mean expression of genes located on the deleted region of chromosome 9 in case #20 (right), chromosome 17 in case #4 (middle), and chromosome 12 in case #5 (left) were -0.15±0.07, -0.37±0.07, and -0.23±0.051 (mean difference ± standard error), respectively. Each spot (black and red, Y-axis) indicates one gene and reflects the difference between each case and the mean of the other cases. Red spots represent genes located on an aberrant chromosome. The X-axis shows the chromosomal location.

were associated with either decreased or increased mRNA expression of genes in that same region, respectively, demonstrating the relationship between chromosomal status and gene expression. From an analysis perspective, we applied a descriptive approach and intended to assess plausibility of data. Some genes do indeed have higher expression values in deleted regions (Figure 4A, red points above zero) than in other cases, and some genes have lower values in trisomy (Figure 4A, red points below zero) than in other cases. However on average, expression in deleted regions is clearly lower than in non-deleted cases.

Because most regions are not recurring, we compared only one sample versus the rest (i.e. case #11 was compared with 37 normal karyotype AML/MDS cases; and cases #20, #4 and #5 were compared with other normal karyotype AML/MDS samples.) Various technical and biological sources of noise can confound the analysis. Overall, expression data appear to be consistent with chromosomal deletions and amplifications of the investigated regions. Further studies in larger cohorts of patients should enable prognostic stratification of patients in relation to their genomic changes and reveal new therapeutic targets.

Authorship and Disclosures

TA performed research, analyzed the data and wrote the paper; SO and MS performed SNP-chip analyses; GY and YN developed the CNAG; NK, AY, CWM and MD assisted in data analyses; SS, CH and TH provided AML samples, performed FISH analysis and aided in data analyses; HPK directed the overall study.

The authors declare no competing financial interests.

References

1. Kelly LM, Gilliland DG. Genetics of myeloid leukemias. Annu Rev Genomics Hum Genet 2002;3:179-98.
2. Estey E, Dohner H. Acute myeloid leukaemia. Lancet 2006;368:1894-907.
3. Erickson P, Gao J, Chang KS, Look T, Whisenant E, Raimondi S, et al. Identification of breakpoints in t(8;21) acute myelogenous leukemia and isolation of a fusion transcript, AML1/ETO, with similarity to Drosophila segmentation gene, runt. Blood 1992;80:1825-31.
4. Miyoshi H, Kozu T, Shimizu K, Enomoto K, Maseki N, Kaneko Y, et al. The t(8;21) translocation in acute myeloid leukemia results in production of an AML1-MTG8 fusion transcript. EMBO J 1993;12:2715-21.
5. Licht JD. AML1 and the AML1-ETO fusion protein in the pathogenesis of t(8;21) AML. Oncogene 2001;20:5660-79.
6. Peterson LF, Zhang DE. The 8;21 translocation in leukemogenesis. Oncogene 2004;23:4255-62.
7. Liu P, Tarlé SA, Hajra A, Claxton DF, Marlton P, Freedman M, et al. Fusion between transcription factor CBF beta/PEBP2 β and a myosin heavy chain in acute myeloid leukemia. Science 1993;261:1041-4.
8. Shigesada K, van de Sluis B, Liu PP. Mechanism of leukemogenesis by the inv(16) chimeric gene CBFB/PEBP2B-MHY11. Oncogene 2004;23:4297-307.
9. de Thé H, Chomienne C, Lanotte M, Degos L, Dejean A. The t(15;17) translocation of acute promyelocytic leukaemia fuses the retinoic acid receptor alpha gene to a novel transcribed locus. Nature 1990;347:558-61.
10. de Thé H, Lavau C, Marchio A, Chomienne C, Degos L, Dejean A. The PML-RAR-α fusion mRNA generated by the t(15;17) translocation in acute promyelocytic leukemia encodes a functionally altered RAR. Cell 1991;66:675-84.
11. Byrd JC, Mrózek K, Dodge RK, Carroll AJ, Edwards CG, Arthur DC, et al. Pretreatment cytogenetic abnormalities are predictive of induction success, cumulative incidence of relapse, and overall survival in adult patients with de novo acute myeloid leukemia: results from Cancer and Leukemia Group B (CALGB 8461). Blood 2002;100:4325-36.
12. Grimwade D, Walker H, Oliver F, Wheatley K, Harrison C, Harrison G, et al. The importance of diagnostic cytogenetics on outcome in AML: analysis of 1,612 patients entered into the MRC AML 10 trial. The Medical Research Council Adult and Children's Leukaemia Working Parties. Blood 1998;92:2322-33.
13. Mrozek K, Marcucci G, Paschka P, Whitman SP, Bloomfield CD. Clinical relevance of mutations and gene-expression changes in adult acute myeloid leukemia with normal cytogenetics: are we ready for a prognostically prioritized molecular classification? Blood 2007;109:431-48.
14. Caligiuri MA, Schichman SA, Strout MP, Mrózek K, Baer MR, Frankel SR, et al. Molecular rearrangement of the ALL-1 gene in acute myeloid leukemia without cytogenetic evidence of 11q23 chromosomal translocations. Cancer Res 1994;54:370-3.
15. Gilliland DG, Griffin JD. The roles of FLT3 in hematopoiesis and leukemia. Blood 2002;100:1532-42.
16. Reuter CW, Morgan MA, Bergmann L. Targeting the Ras signaling pathway: a rational, mechanism-based treatment for hematologic malignancies? Blood 2000;96:1655-69.
17. Pabst T, Mueller BU, Zhang P, Radomska HS, Narravula S, Schnittger S, et al. Dominant-negative mutations of CEBPA, encoding CCAAT/enhancer binding protein-alpha (C/EBPα), in acute myeloid leukemia. Nat Genet 2001;27:263-70.
18. Gombart AF, Hofmann WK, Kawano S, Takeuchi S, Krug U, Kwok SH, et al. Mutations in the gene encoding the transcription factor CCAAT/enhancer binding protein alpha in myelodysplastic syndromes and acute myeloid leukemias. Blood 2002;99:1332-40.
19. Falini B, Mecucci C, Tiacci E, Alcalay M, Rosati R, Pasqualucci L, et al. Cytoplasmic nucleophosmin in acute myelogenous leukemia with a normal karyotype. N Engl J Med 2005;352:254-66.
20. Falini B, Nicoletti I, Martelli MF, Mecucci C. Acute myeloid leukemia carrying cytoplasmic/mutated nucleophosmin (NPMc+ AML): biologic and clinical features. Blood 2007;109:874-85.
21. Nannya Y, Sanada M, Nakazaki K, Hosoya N, Wang L, Hangaishi A, et al. A robust algorithm for copy number detection using high-density oligonucleotide single nucleotide polymorphism genotyping arrays. Cancer Res 2005;65:6071-9.
22. Engle LJ, Simpson CL, Landers JE. Using high-throughput SNP technologies to study cancer. Oncogene 2006;25:1594-601.
23. Yamamoto G, Nannya Y, Kato M, Sanada M, Levine RL, Kawamata N, et al. Highly sensitive method for genomewide detection of allelic composition in nonpaired, primary tumor specimens by use of affymetrix single-nucleotide-polymorphism genotyping microarrays. Am J Hum Genet 2007;81:114-26.
24. Pfeifer D, Pantic M, Skatulla I, Rawluk J, Kreutz C, Martens UM, et al. Genome-wide analysis of DNA copy number changes and LOH in

CLL using high-density SNP arrays. Blood 2007;109:1202-10.
25. Lehmann S, Ogawa S, Raynaud SD, Sanada M, Nannya Y, Ticchioni M, et al. Molecular allelokaryotyping of early stage untreated chronic lymphocytic leukemia. Cancer 2008; 112:1296-305.
26. Mullighan CG, Goorha S, Radtke I, Miller CB, Coustan-Smith E, Dalton JD, et al. Genome-wide analysis of genetic alterations in acute lymphoblastic leukaemia. Nature 2007; 446:758-64.
27. Kawamata N, Ogawa S, Zimmermann M, Kato M, Sanada M, Hemminki K, et al. Molecular allelokaryotyping of pediatric acute lymphoblastic leukemias by high resolution single nucleotide polymorphism oligonucleotide genomic microarray. Blood 2008;111:776-84.
28. Flotho C, Steinemann D, Mullighan CG, Neale G, Mayer K, Kratz CP, et al. Genome-wide single-nucleotide polymorphism analysis in juvenile myelomonocytic leukemia identifies uniparental disomy surrounding the NF1 locus in cases associated with neurofibromatosis but not in cases with mutant RAS or PTPN11. Oncogene 2007;26:5816-21.
29. Fitzgibbon J, Iqbal S, Davies A, O'shea D, Carlotti E, Chaplin T, et al. Genome-wide detection of recurring sites of uniparental disomy in follicular and transformed follicular lymphoma. Leukemia 2007;21:1514-20.
30. Walker BA, Leone PE, Jenner MW, Li C, Gonzalez D, Johnson DC, et al. Integration of global SNP-based mapping and expression arrays reveals key regions, mechanisms, and genes important in the pathogenesis of multiple myeloma. Blood 2006;108:1733-43.
31. Raghavan M, Lillington DM, Skoulakis S, Debernardi S, Chaplin T, Foot NJ, et al. Genome-wide single nucleotide polymorphism analysis reveals frequent partial uniparental disomy due to somatic recombination in acute myeloid leukemias. Cancer Res 2005;65:375-8.
32. Fitzgibbon J, Smith LL, Raghavan M, Smith ML, Debernardi S, Skoulakis S, et al. Association between acquired uniparental disomy and homozygous gene mutation in acute myeloid leukemias. Cancer Res 2005;65:9152-4.
33. Tyybäkinoja A, Elonen E, Piippo K, Porkka K, Knuutila S. Oligonucleotide array-CGH reveals cryptic gene copy number alterations in karyotypically normal acute myeloid leukemia. Leukemia 2007;21:571-4.
34. Kiyoi H, Naoe T, Yokota S, Nakao M, Minami S, Kuriyama K, et al. Internal tandem duplication of FLT3 associated with leukocytosis in acute promyelocytic leukemia: Leukemia Study Group of the Ministry of Health and Welfare (Kohseisho). Leukemia 1997;11: 1447-52.
35. Schnittger S, Schoch C, Dugas M, Kern W, Staib P, Wuchter C, et al. Analysis of FLT3 length mutations in 1003 patients with acute myeloid leukemia: correlation to cytogenetics, FAB subtype, and prognosis in the AMLCG study and usefulness as a marker for the detection of minimal residual disease. Blood 2002; 100:59-66.
36. Schnittger S, Schoch C, Kern W, Mecucci C, Tschulik C, Martelli MF, et al. Nucleophosmin gene mutations are predictors of favorable prognosis in acute myelogenous leukemia with a normal karyotype. Blood 2005;106:3733-9.
37. Dicker F, Haferlach C, Kern W, Haferlach T, Schnittger S. Trisomy 13 is strongly associated with AML1/RUNX1 mutations and increased FLT3 expression in acute myeloid leukemia. Blood 2007;110: 1308-16.
38. Yin D, Xie D, Hofmann WK, Miller CW, Black KL, Koeffler HP. Methylation, expression, and mutation analysis of the cell cycle control genes in human brain tumors. Oncogene 2002;21:8372-8.
39. Bolstad BM, Irizarry RA, Astrand M, Speed TP. A comparison of normalization methods for high density oligonucleotide array data based on variance and bias. Bioinformatics 2003;19:185-93.
40. Haferlach T, Kohlmann A, Schnittger S, Dugas M, Hiddemann W, Kern W, et al. A global approach to the diagnosis of leukemia using gene expression profiling. Blood 2005;106:1189-98.
41. Hemann MT, Bric A, Teruya-Feldstein J, Herbst A, Nilsson JA, Cordon-Cardo C, et al. Evasion of the p53 tumour surveillance network by tumour-derived MYC mutants. Nature 2005;436:807-11.
42. Dang CV, O'Donnell KA, Juopperi T. The great MYC escape in tumorigenesis. Cancer Cell 2005;8:177-8.
43. Baxter EJ, Scott LM, Campbell PJ, East C, Fourouclas N, Swanton S, et al. Acquired mutation of the tyrosine kinase JAK2 in human myeloproliferative disorders. Lancet 2005; 365:1054-61.
44. Lee JW, Kim YG, Soung YH, Han KJ, Kim SY, Rhim HS, et al. The JAK2 V617F mutation in de novo acute myelogenous leukemias. Oncogene 2006;25:1434-6.
45. Illmer T, Schaich M, Ehninger G, Thiede C; DSIL2003 AML study group. Tyrosine kinase mutations of JAK2 are rare events in AML but influence prognosis of patients with CBF-leukemias. Haematologica 2007; 92:137-8.
46. Side LE, Emanuel PD, Taylor B, Franklin J, Thompson P, Castleberry RP, et al. Mutations of the NF1 gene in children with juvenile myelomonocytic leukemia without clinical evidence of neurofibromatosis, type 1. Blood 1998;92:267-72.
47. Hernández JM, González MB, García JL, Ferro MT, Gutiérrez NC, Marynen P, et al. Two cases of myeloid disorders and a t(8;12)(q12;p13). Haematologica 2000;85: 31-4.
48. Barjesteh van Waalwijk van Doorn-Khosrovani S, Spensberger D, de Knegt Y, Tang M, Löwenberg B, Delwel R. Somatic heterozygous mutations in ETV6 (TEL) and frequent absence of ETV6 protein in acute myeloid leukemia. Oncogene 2005;24:4129-37.
49. R Development Core Team. R: A language and environment for statistical computing. R Foundation for Statistical Computing, Vienna, Austria. 2007; ISBN 3-900051-07-0.
50. Serrano E, Carnicer MJ, Orantes V, Estivill C, Lasa A, Brunet S, et al. Uniparental disomy may be associated with microsatellite instability in acute myeloid leukemia (AML) with a normal karyotype. Leuk Lymphoma 2008;49:1178-83.
51. Gupta M, Raghavan M, Gale RE, Chelala C, Allen C, Molloy G, et al. Novel regions of acquired uniparental disomy discovered in acute myeloid leukemia. Genes Chromosomes Cancer 2008;47:729-39.
52. Raghavan M, Smith LL, Lillington DM, Chaplin T, Kakkas I, Molloy G, et al. Segmental uniparental disomy is a commonly acquired genetic event in relapsed acute myeloid leukemia. Blood 2008;112:814-21.
53. Gorletta TA, Gasparini P, D'Elios MM, Trubia M, Pelicci PG, Di Fiore PP. Frequent loss of heterozygosity without loss of genetic material in acute myeloid leukemia with a normal karyotype. Genes Chromosomes Cancer 2005;44: 334-7.
54. Tyybäkinoja A, Elonen E, Vauhkonen H, Saarela J, Knuutila S. Single nucleotide polymorphism microarray analysis of karyotypically normal acute myeloid leukemia reveals frequent copy number neutral loss of heterozygosity. Haematologica 2008; 93:631-2.

nature Vol 460|13 August 2009|doi:10.1038/nature08240

LETTERS

Gain-of-function of mutated *C-CBL* tumour suppressor in myeloid neoplasms

Masashi Sanada[1,5]*, Takahiro Suzuki[7]*, Lee-Yung Shih[8]*, Makoto Otsu[9], Motohiro Kato[1,2], Satoshi Yamazaki[6], Azusa Tamura[1], Hiroaki Honda[11], Mamiko Sakata-Yanagimoto[12], Keiki Kumano[3], Hideaki Oda[13], Tetsuya Yamagata[14], Junko Takita[1,2,3], Noriko Gotoh[10], Kumi Nakazaki[1,4], Norihiko Kawamata[15], Masafumi Onodera[16], Masaharu Nobuyoshi[7], Yasuhide Hayashi[17], Hiroshi Harada[18], Mineo Kurokawa[3,4], Shigeru Chiba[12], Hiraku Mori[18], Keiya Ozawa[7], Mitsuhiro Omine[18], Hisamaru Hirai[3,4], Hiromitsu Nakauchi[6,9], H. Phillip Koeffler[15] & Seishi Ogawa[1,5]

Acquired uniparental disomy (aUPD) is a common feature of cancer genomes, leading to loss of heterozygosity. aUPD is associated not only with loss-of-function mutations of tumour suppressor genes[1], but also with gain-of-function mutations of proto-oncogenes[2]. Here we show unique gain-of-function mutations of the *C-CBL* (also known as *CBL*) tumour suppressor that are tightly associated with aUPD of the 11q arm in myeloid neoplasms showing myeloproliferative features. The *C-CBL* proto-oncogene, a cellular homologue of *v-Cbl*, encodes an E3 ubiquitin ligase and negatively regulates signal transduction of tyrosine kinases[3–6]. Homozygous *C-CBL* mutations were found in most 11q-aUPD-positive myeloid malignancies. Although the *C-CBL* mutations were oncogenic in NIH3T3 cells, c-Cbl was shown to functionally and genetically act as a tumour suppressor. C-CBL mutants did not have E3 ubiquitin ligase activity, but inhibited that of wild-type C-CBL and CBL-B (also known as CBLB), leading to prolonged activation of tyrosine kinases after cytokine stimulation. *c-Cbl*$^{-/-}$ haematopoietic stem/progenitor cells (HSPCs) showed enhanced sensitivity to a variety of cytokines compared to *c-Cbl*$^{+/+}$ HSPCs, and transduction of *C-CBL* mutants into *c-Cbl*$^{-/-}$ HSPCs further augmented their sensitivities to a broader spectrum of cytokines, including stem-cell factor (SCF, also known as KITLG), thrombopoietin (TPO, also known as THPO), IL3 and FLT3 ligand (FLT3LG), indicating the presence of a gain-of-function that could not be attributed to a simple loss-of-function. The gain-of-function effects of C-CBL mutants on cytokine sensitivity of HSPCs largely disappeared in a *c-Cbl*$^{+/+}$ background or by co-transduction of wild-type *C-CBL*, which suggests the pathogenic importance of loss of wild-type *C-CBL* alleles found in most cases of *C-CBL*-mutated myeloid neoplasms. Our findings provide a new insight into a role of gain-of-function mutations of a tumour suppressor associated with aUPD in the pathogenesis of some myeloid cancer subsets.

Myelodysplastic syndromes (MDS) are heterogeneous groups of blood cancers originating from haematopoietic precursors. They are characterized by deregulated haematopoiesis showing a high propensity to acute myeloid leukaemia (AML)[7]. Some MDS cases have overlapping clinico-pathological features with myeloproliferative disorders, and are now classified into myelodysplasia/myeloproliferative neoplasms (MDS/MPN) by the World Health Organization (WHO) classification[8]. To obtain a comprehensive profile of allelic imbalances in these myeloid neoplasms, we performed allele-specific copy number analyses of bone marrow samples obtained from 222 patients with MDS, MDS/MPN, or other related myeloid neoplasms (Supplementary Tables 1 and 2) using high-density single nucleotide polymorphism (SNP) arrays combined with CNAG/AsCNAR software[9,10].

Genomic profiles of MDS and MDS/MPN showed characteristic unbalanced genetic changes, as reported in previous cytogenetic studies[11] (Supplementary Fig. 1a); however, they were detected more sensitively by SNP array analyses (Supplementary Table 3). aUPD was detected in 70 samples (31.5%) on the basis of the allele-specific copy number analyses, which substantially exceeded the detection rate obtained using a SNP call-based detection algorithm (20.7%) (Supplementary Figs 2 and 4, and Supplementary Tables 4 and 5). Long stretches of homozygous SNP calls caused by shared identical-by-descent alleles in parents were empirically predicted and excluded (Supplementary Fig. 3). aUPDs were more common in MDS/MPN than in MDS. They preferentially affected several chromosomal arms (1p, 1q, 4q, 7q, 11p, 11q, 14q, 17p and 21q) in distinct subsets of patients, and frequently associated with mutated oncogenes and tumour suppressor genes (Supplementary Figs 1b and 5). Among these, the most common aUPDs were those involving 11q ($n = 17$), which defined a unique subset of myeloid neoplasms that were clinically characterized by frequent diagnosis of chronic myelomonocytic leukaemia (CMML) with normal karyotypes (13 cases) (Fig. 1a and Supplementary Table 6). We identified a minimum overlapping aUPD segment of approximately 1.4 megabases (Mb) in 11q, which contained a mutated *C-CBL* proto-oncogene (Fig. 1b).

[1]Cancer Genomics Project, [2]Department of Pediatrics, [3]Cell Therapy and Transplantation Medicine, and [4]Hematology and Oncology, Graduate School of Medicine, The University of Tokyo, 7-3-1 Hongo, Bunkyo-ku, Tokyo 113-8655, Japan. [5]Core Research for Evolutional Science and Technology, [6]Exploratory Research for Advanced Technology, Japan Science and Technology Agency, 4-1-8 Honcho, Kawaguchi-shi, Saitama 332-0012, Japan. [7]Division of Hematology, Department of Medicine, Jichi Medical University, 3311-1 Yakushiji, Shimotsuke-shi, Tochigi 329-0498, Japan. [8]Division of Hematology-Oncology, Department of Internal Medicine, Chang Gung Memorial Hospital, Chang Gung University, 199 Tung Hwa North Road, Taipei 105, Taiwan. [9]Division of Stem Cell Therapy, Center for Stem Cell and Regenerative Medicine, [10]Division of Systems Biomedical Technology, Institute of Medical Science, The University of Tokyo, 4-6-1 Shirokanedai, Minato-ku, Tokyo 108-8639, Japan. [11]Department of Developmental Biology, Research Institute of Radiation Biology and Medicine, Hiroshima University, 1-2-3 Kasumi, Minami-ku, Hiroshima 734-8553, Japan. [12]Department of Clinical and Experimental Hematology, Institute of Clinical Medicine, University of Tsukuba, 1-1-1 Tennodai, Tukuba-shi, Ibaraki, 305-8571, Japan. [13]Department of Pathology, Tokyo Women's Medical University, 8-1 Kawada-cho, Shinjuku-ku, Tokyo 162-8666, Japan. [14]Department of Hematology, Dokkyo University School of Medicine, 800 Kitabayashi, Mibu, Tochigi 321-0293, Japan. [15]Hematology/Oncology, Cedars-Sinai Medical Center, 8700 Beverly Boulevard, Los Angeles, California 90048, USA. [16]Department of Genetics, National Research Institute for Child Health and Development, 2-10-1 Okura, Setagaya-ku, Tokyo, 157-8535, Japan. [17]Gunma Children's Medical Center, 779 Shimohakoda, Hokkitsu-machi, Shibukawa-shi, Gunma 377-8577, Japan. [18]Division of Hematology, Internal Medicine, Showa University Fujigaoka Hospital, 1-30 Fujigaoka, Aoba-ku, Yokohama, Kanagawa 227-8501, Japan.
*These authors contributed equally to this work.

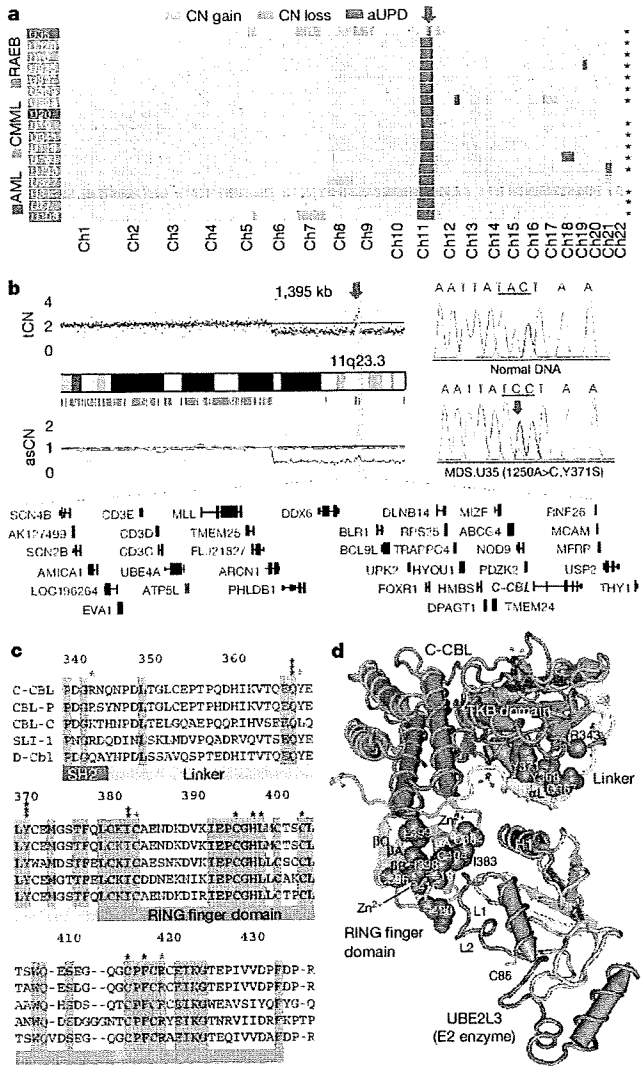

Figure 1 | Common UPD on the 11q arm and *C-CBL* mutations in myeloid neoplasms. a, Copy number profiles of 17 cases with myeloid neoplasms showing 11qUPD. Regions of copy number (CN) gains, losses and aUPD are depicted in different colours. Histologies are shown by coloured boxes. Asterisks denote *C-CBL*-mutated cases. Ch, chromosome; RAEB, refractory anaemia with excess blasts. **b**, CNAG output for MDS.U35. Total copy number (tCN) and allele-specific copy number (asCN) plots show a focal copy number gain spanning a 1.4-Mb segment within 3 Mb of an 11q-aUPD region (left), which contained mutated *C-CBL* in MDS.U35 (right). **c**, Alignments of amino acid sequences for human CBL family proteins and their homologues in *Caenorhabditis elegans* (SLI-1) and *Drosophila* (D-Cbl). Amino acid numbering is on the basis of human *C-CBL*. Conserved amino acids are highlighted. Positions of mutated amino acids are indicated by asterisks. Heterozygous mutations are shown in red. **d**, Mutated amino acid positions in the three-dimensional structure of a human C-CBL–UBE2L3 complex. TKB, tyrosine kinase binding domain.

C-CBL is the cellular homologue of the *v-Cbl* transforming gene of the Cas NS-1 murine leukaemia virus[5,12]. It was recently found to be mutated in human AML cases[13–15]. Together with its close homologue, CBL-B, C-CBL is thought to be involved in the negative modulation of tyrosine kinase signalling, primarily through their E3 ubiquitin ligase activity that is responsible for the downregulation of activated tyrosine kinases[3–5]. By sequencing all *C-CBL* exons in all 222 samples, we found *C-CBL* mutations in 15 of the 17 cases with 11q-aUPD, whereas only 3 out of 205 cases without 11q-aUPD had *C-CBL* mutations, showing a strong association of *C-CBL* mutations with 11q-aUPD ($P = 1.46 \times 10^{-18}$) (Supplementary Fig. 6 and Supplementary Tables 6 and 7), as also indicated in a recent report[16]. Thus, *C-CBL* was thought to be the major, if not the only, target of 11q-aUPD in myeloid neoplasms. Two different *C-CBL* mutations co-existed in three cases (Supplementary Fig. 6b). Somatic origins of the mutations were confirmed in three evaluable cases (Supplementary Fig. 6c).

In most cases, *C-CBL* mutations were missense, involving the evolutionarily conserved amino acids within the linker-RING finger domain that is central to the E3 ubiquitin ligase activity[17] (Fig. 1c). Another case with a predominant Cys384Tyr mutation also contained a nonsense mutation (Arg343X) in a minor subclone, which resulted in a v-Cbl-like truncated protein (Supplementary Fig. 6b). In the remaining two cases, mutations led to amino acid deletions (Δ369−371 and Δ368−382) involving the highly conserved α-helix (αL) of the linker domain and the first loop of the RING finger. According to the published crystal structure of *C-CBL*[17], most of the mutated or deleted amino acids were positioned on the interface for the binding to the E2 enzyme (Fig. 1d), making contact with either the tyrosine kinase binding domain (Tyr 368 and Tyr 371) or E2 ubiquitin-conjugating enzymes (Ile 383, Cys 404 and Phe 418). Especially, all seven linker-domain mutations selectively involved just three amino acids (Gln 367, Tyr 368 and Tyr 371) within the conserved αL helix (Fig. 1d). Mutations were clearly homozygous in nine cases, and the apparently heterozygous chromatograms in the other six cases could also be compatible with homozygous mutations affecting the aUPD-positive tumour clones, given the presence of substantial normal cell components within these samples. Mutations in the remaining three cases were considered to be heterozygous. About half of the *C-CBL*-mutated cases carried coexisting mutations of *RUNX1* (four cases), *TP53* (one case), *FLT3* internal tandem duplication (1 case) or *JAK2* (3 cases). *NRAS* and *KRAS* mutations were prevalent among CMML (15.1%) but occurred within discrete clusters from *C-CBL*-mutated cases (Supplementary Tables 2 and 6 and Supplementary Fig. 5). The mutation status of *C-CBL* did not substantially affect the clinical outcome (Supplementary Fig. 7).

All tested *C-CBL* mutants induced clear oncogenic phenotypes in NIH3T3 fibroblasts, as demonstrated by enhanced colony formation in soft agar and tumour generation in nude mice (Supplementary Fig. 8). Transformed NIH3T3 cells showed PI3 kinase-dependent activation of Akt and the transformed phenotype was reverted by treatment with the PI3 kinase inhibitor Ly294002 (Supplementary Fig. 9). When introduced into Lin^- $Sca1^+$ c-Kit^+ (LSK) HSPCs, C-CBL mutants (C-CBL(Gln367Pro) and C-CBL(Tyr371Ser)), as well as a mouse lymphoma-derived oncogenic mutant (C-CBL(70Z)), significantly promoted the replating capacity of these progenitors (Fig. 2a). Because c-Cbl negatively modulates tyrosine kinase signalling, and all *C-CBL* mutations, including those previously reported[13–16], affected the critical domains for its enzymatic activity involved in this modulation, C-CBL was postulated to have a tumour suppressor function; loss-of-function could be a mechanism for the oncogenicity of these C-CBL mutants[3,5]. To assess this possibility and to clarify further the role of *C-CBL* mutations in the pathogenesis of myeloid neoplasms, we generated *c-Cbl*$^{-/-}$ mice and examined their haematological phenotypes (Supplementary Fig. 10).

In agreement with previous reports[18–20], *c-Cbl*$^{-/-}$ mice exhibited splenomegaly and an augmented haematopoietic progenitor pool, as was evident from the increased colony formation of bone marrow cells in methylcellulose culture and higher numbers of LSK and CD34-negative LSK cells in bone marrow and/or spleen compared to their wild-type littermates (Fig. 2b–d and Supplementary Fig. 11). Furthermore, when introduced into a *BCR-ABL* transgenic background[21], the *c-Cbl*$^{-/-}$ allele accelerated blastic crisis depending on the allele dosage (Fig. 2e, f). These observations supported the notion that wild-type *C-CBL* has tumour suppressor functions, whereas 'mutant' *C-CBL* acts as an oncogene; *C-CBL* can therefore be both a proto-oncogene and a tumour suppressor gene.

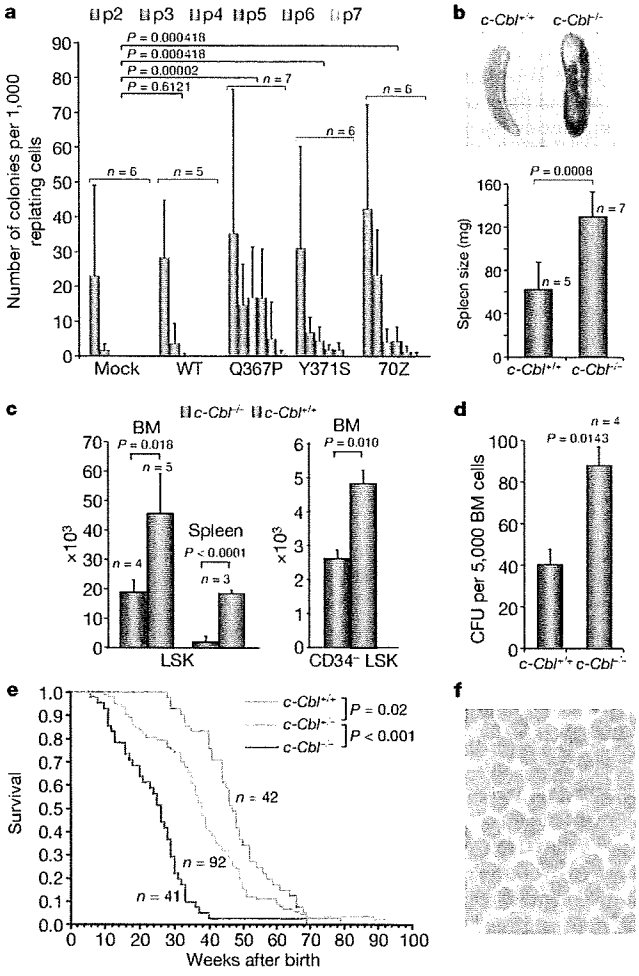

Figure 2 | Tumour-suppressor functions of wild-type C-CBL. **a**, Prolonged replating capacity of LSK cells transduced with mutant *C-CBL* (*C-CBL*(Gln367Pro) and *C-CBL*(Tyr371Ser)), compared to mock- or wild-type *C-CBL*-transduced cells. Replating capacity in methylcellulose culture is shown as mean colony number (and s.d.) per 1,000 replating cells at indicated times of replating. p, passage. **b**, Increased spleen mass in *c-Cbl*$^{-/-}$ mice compared to *c-Cbl*$^{+/+}$ mice (mean spleen weight and s.d.). **c**, Mean number of total LSK (left) and CD34-negative LSK (right) cells (plus s.d.) in bone marrow (BM) and/or spleen in *c-Cbl*$^{+/+}$ (blue columns) and *c-Cbl*$^{-/-}$ mice (red columns). Bone marrow cells from bilateral tibias and femurs were counted for each mouse. **d**, Augmented colony-forming potential of bone marrow cells from *c-Cbl*$^{-/-}$ mice (mean colony number and s.d. per 5,000 bone marrow cells). CFU, colony-forming units. **e**, Kaplan–Meier survival curves of *c-Cbl*$^{+/+}$, *c-Cbl*$^{+/-}$ and *c-Cbl*$^{-/-}$ mice carrying a *BCR-ABL* transgene, showing acceleration of blastic crisis in *c-Cbl*$^{+/-}$ and *c-Cbl*$^{-/-}$ mice. **f**, Wright–Giemsa staining of an enlarged lymph node in a *Bcr-Abl*$^{+}$ *c-Cbl*$^{-/-}$ mouse during blastic crisis shows massive infiltrates of immature leukaemic blasts. Original magnification, ×600.

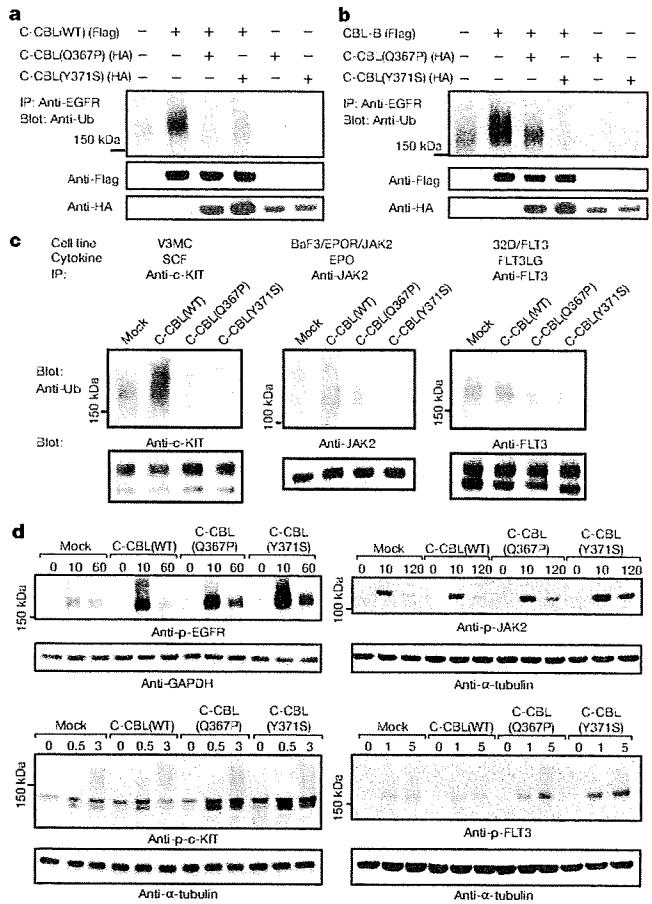

Figure 3 | Inhibitory actions of C-CBL mutants on wild-type C-CBL. **a**, **b**, Flag-tagged wild-type C-CBL (**a**) or CBL-B (**b**) were transfected into NIH3T3 cells stably transduced with human EGFR plus indicated HA-tagged C-CBL mutants. Anti-ubiquitin blots of immunoprecipitated EGFR after EGF stimulation show the inhibitory actions of the C-CBL mutants on ubiquitinating activity of C-CBL (**a**) and CBL-B (**b**). Bottom panels are anti-HA and anti-Flag blots of total cell lysates. **c**, Effects of wild-type and mutant C-CBL on cytokine-induced ubiquitination of c-KIT, JAK2 and FLT3 in haematopoietic cells V3MC, BaF3 co-transduced with human erythropoietin receptor (EPOR) and JAK2 (BaF3/EPOR/JAK2), and FLT3-transduced 32D (32D/FLT3), respectively. Each cell line was further transduced with indicated C-CBL mutants, and ubiquitination of immunoprecipitated kinases was detected by anti-ubiquitin blots at 1 min after stimulation with SCF, EPO and FLT3LG. Anti-kinase blots of the precipitated kinases are shown below each panel. **d**, Kinase phosphorylation was examined at indicated time points (shown in minutes) after ligand stimulation using immunoblot analyses of total cell lysates using antibodies to phosphorylated (p-) EGFR, c-KIT, JAK2 and FLT3 in which anti-α-tubulin or anti-GAPDH blots are provided as a control.

Mouse LSK HSPCs expressed two Cbl family member proteins: wild-type c-Cbl and Cbl-b (Supplementary Fig. 12)[22]. When transduced into NIH3T3 cells stably expressing human epidermal growth factor receptor (EGFR), both Cbl proteins enhanced ubiquitination of EGFR after EGF stimulation, which was suppressed by coexpression of the C-CBL mutants (Fig. 3a, b). In haematopoietic cells, overexpression of wild-type C-CBL enhanced ligand-induced ubiquitination of a variety of tyrosine kinases, including c-KIT, FLT3 and JAK2. In contrast, C-CBL mutants not only showed compromised enzymatic activity, but also inhibited the ubiquitinating activities in these haematopoietic cells (Fig. 3c), leading to prolonged tyrosine kinase activation after ligand stimulation (Fig. 3d).

Because tyrosine kinase signalling is central to cytokine responses in haematopoietic cells and its deregulation is a common feature of myeloproliferative disorders[23], we next examined the effects of *C-CBL* mutations (*C-CBL*(Gln367Pro) and *C-CBL*(Tyr371Ser)) and the loss of wild-type *C-CBL* alleles on the responses of LSK HSPCs to various cytokines. In serum-free conditions, *c-Cbl*$^{-/-}$ LSK cells showed a modestly enhanced proliferative response to a variety of cytokines, including SCF, IL3 and TPO, compared to *c-Cbl*$^{+/+}$ cells (mock columns in Fig. 4a). However, the enhanced response in *c-Cbl*$^{-/-}$ cells was markedly augmented and extended to a broader spectrum of cytokines, including FLT3 ligand by the transduction of *C-CBL* mutants. Of note, the effect of *C-CBL* mutant transduction was not remarkable in *c-Cbl*$^{+/+}$ LSK cells except for the response to SCF, which was clearly enhanced by *C-CBL* mutants

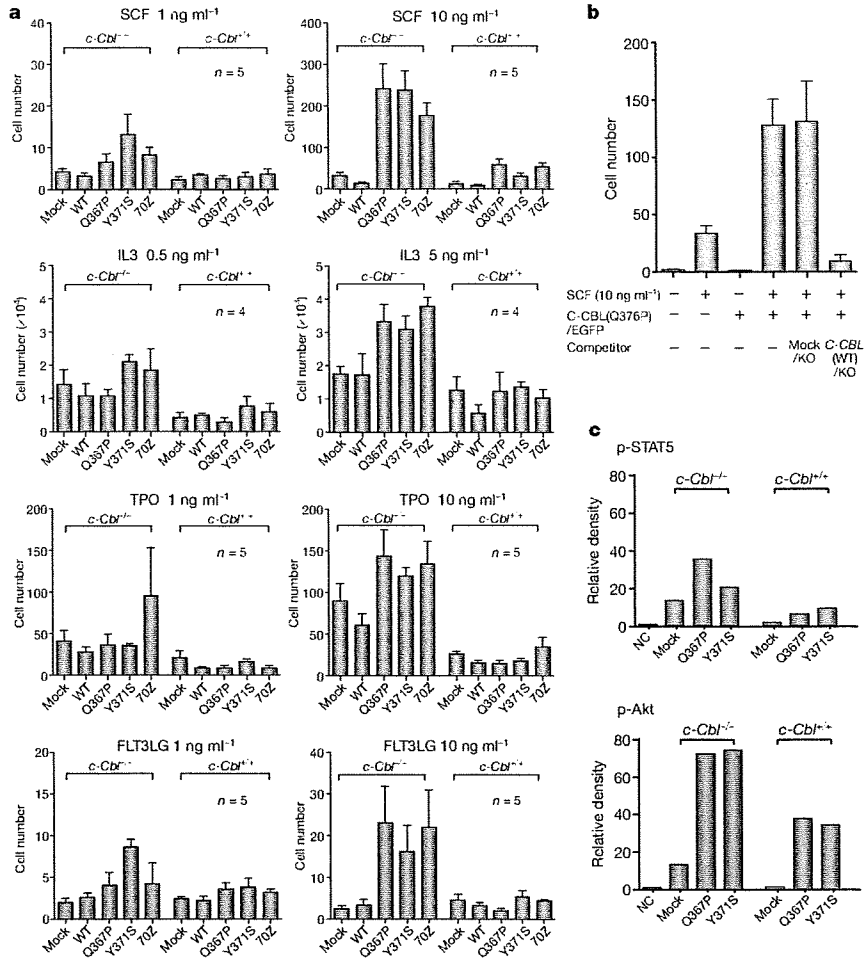

Figure 4 | Gain-of-function of mutant C-CBL augmented by loss of wild-type C-CBL. a, *c-Cbl*$^{+/+}$ and *c-Cbl*$^{-/-}$ LSK cells were transfected with various *C-CBL* internal ribosome entry site (IRES)/green fluorescent protein (GFP) constructs, and 50 GFP-positive cells were sorted for serum-free culture containing indicated concentrations of SCF, IL3, TPO and FLT3LG. Mean cell numbers (plus s.e.m.) on day 5 are plotted. **b**, *c-Cbl*$^{-/-}$ LSK cells were co-transduced with C-CBL(Gln367Pro)-IRES-EGFP (C-CBL(Q367P)/EGFP) and mock-IRES-Kusabira-Orange (mock/KO) or wild-type *C-CBL*-IRES-Kusabira-Orange (*C-CBL*(WT)/KO), and 50 GFP/KO double-positive cells were sorted into each well for cell proliferation assays in serum-free culture containing 10 ng ml^{-1} SCF. Mean cell numbers on day 5 (plus s.e.m., $n = 5$) are plotted. **c**, Ten thousand *c-Cbl*$^{+/+}$ and *c-Cbl*$^{-/-}$ LSK cells transduced with various C-CBL constructs were stimulated with 10 ng ml^{-1} SCF and 10 ng ml^{-1} TPO for 15 min. Total cell lysates were analysed by immunoblotting, using antibodies to STAT5, Akt and their phosphorylated forms. The intensities of phosphorylated proteins relative to total STAT5 (top panel) and Akt (bottom panel) are plotted. NC indicates the mean background signal obtained with nonspecific IgG.

even with a *c-Cbl*$^{+/+}$ background (Fig. 4a and Supplementary Fig. 13). To clarify further the effect of wild-type C-CBL on C-CBL mutants, both wild-type C-CBL and C-CBL mutants were co-transduced into *c-Cbl*$^{-/-}$ LSK cells, and their effects on the response to SCF were examined. As shown in Fig. 4b, the hyperproliferative response induced by C-CBL mutants was almost completely abolished by the co-transduction of wild-type C-CBL, suggesting the pathogenic importance of loss of wild-type *C-CBL* alleles found in most *C-CBL*-mutated cases. LSK cells transduced with C-CBL mutants also showed enhanced activation of the STAT5 and Akt pathways on cytokine stimulation (SCF and TPO), which was more pronounced in *c-Cbl*$^{-/-}$ than *c-Cbl*$^{+/+}$ LSK cells (Fig. 4c and Supplementary Fig. 14).

The modest enhancement of sensitivity to cytokines found in *c-Cbl*$^{-/-}$ LSK cells was a consequence of loss of C-CBL functions. In contrast, the hypersensitive response of mutant-transduced *c-Cbl*$^{-/-}$ LSK cells to a broad spectrum of cytokines represents gain-of-function of the mutants that could not be ascribed to a simple loss of C-CBL functions, which was also predicted from the strong association of *C-CBL* mutations with 11q-aUPD by analogy to the gain-of-function *JAK2* mutations associated with 9p-aUPD in polycythemia vera[2]. The gain-of-function of C-CBL mutants became more evident under a *c-Cbl*$^{-/-}$ background. The hypersensitive response to cytokines induced by mutant C-CBL under the *c-Cbl*$^{-/-}$ background was largely offset by the presence of the wild-type *c-Cbl* allele or by the transduction of the wild-type C-CBL gene, suggesting that the gain-of-function could be closely related to loss of C-CBL-like functions, probably by inhibition of Cbl-b. Supporting this view is a previous report that *c-Cbl/Cbl-b* double knockout T cells showed more profound impairments in the downregulation of the T-cell receptor (TCR), more sustained TCR signalling, and more vigorous proliferation, than *c-Cbl* or *Cbl-b* single knockout T cells after anti-CD3 (also known as CD3e) stimulation[24]. This is analogous to the gain-of-function found in some TP53 mutants, which has been explained by functional inhibition of two TP53 homologues, TP73 and TP63 (refs 25, 26). Of note, TP53 was also originally isolated as an oncogene through its mutated forms[27]. The Cbl-b inhibition-based gain-of-function model could be tested directly by comparing the behaviour of *c-Cbl/Cbl-b* double knockout LSK cells with that of LSK cells carrying homozygously knocked-in mutant *C-CBL* alleles. On the other hand, there remains a possibility that the gain-of-function could be mediated by a mechanism other than the simple inhibition of the homologue, because C-CBL mutants retained several motifs